Article

Heat-Resistant Polymers with Intense, Visible Photoluminescence Functionality and Fluorescence Probing Application

Masatoshi Hasegawa *[ID] **and Shunichi Horii**

Department of Chemistry, Faculty of Science, Toho University, 2-2-1 Miyama, Funabashi 274-8510, Chiba, Japan
* Correspondence: mhasegaw@chem.sci.toho-u.ac.jp

Abstract: Heat-resistant polymers with an intense, visible photoluminescence (PL) functionality are presented. A polybenzoxazole (PBO) containing hexafluoroisopropylidene (HFIP) side groups exhibited an intense purple PL with a quantum yield, Φ_{PL}, of 0.22 (22%), owing to the effectively disturbed concentration quenching (CQ) in the fluorophore units by the bulky HFIP side groups. The chain ends of a wholly cycloaliphatic polyimide (PI), derived from 1,2,3,4-cyclobutanetetracarboxylic dianhydride (CBDA) and 4,4′-methylenebis(cyclohexylamine) (MBCHA), were modified with conjugated monoamines. The PI derived from 2,3,6,7-naphthalenetetracarboxylic dianhydride (2,3,6,7-NTDA) and MBCHA exhibited a very high glass transition temperature (T_g = 376 °C) and purple fluorescence from the $S_1(\pi,\pi^*)$ state. However, its Φ_{PL} value was lower than expected. A pronounced effect of fluorophore dilution using CBDA on the PL enhancement was observed. This is closely related to the planar structure of the 2,3,6,7-NTDA-based diimide units. By contrast, the counterpart using an 2,3,6,7-NTDA isomer, 1,4,5,8-NTDA, was virtually non-fluorescent, despite its sufficient dilution using CBDA. The PI film obtained using 3,3″,4,4″-*p*-terphenyltetracarboxylic dianhydride (TPDA) with a non-coplanar structure and MBCHA exhibited an intense blue fluorescence spectrum (Φ_{PL} = 0.26) peaking at 434 nm. The dilution approach using CBDA enhanced its fluorescence up to a high Φ_{PL} value of 0.41. Even when TPDA was combined with an aromatic diamine, 2,2′-bis(trifluoromethyl)benzidine (TFMB), the intense blue fluorescence was observed without charge-transfer fluorescence. A semi-cycloaliphatic PI derived from TFMB and a novel cycloaliphatic tetracarboxylic dianhydride, which was obtained from a hydrogenated trimellitic anhydride derivative and 4,4′-biphenol, was used as another host polymer for 9,10-bis(4-aminophenyl)anthracene (BAPA). The BAPA-incorporating PI film resulted in a significant PL enhancement with a considerably high Φ_{PL} of 0.48. This PI film also had a relatively high T_g (265 °C). A reactive dye, *N,N′*-bis[4-(4-amino-3-methylbenzyl)-2-methylphenyl]-3,4,9,10-perylenetetracarboxydiimide, was harnessed as a fluorescence probe to explore transamidation between polyimide precursors in solution.

Keywords: heat-resistant polymers; photoluminescence; polyimides; polybenzoxazoles; polyazomethines; concentration quenching; vibronic structure; mirror image; fluorescence probe; transamidation

1. Introduction

Heat-resistant polymers are indispensable as electrically insulating films in the fields of electronics. Among them, aromatic polyimides (PIs) and aromatic polybenzazoles, including polybenzoxazoles (PBOs), polybenzimidazoles, and polybenzthiazoles, are known to have the highest heat resistance [1]. In particular, aromatic PIs have been applied in various electronic devices owing to their simple manufacturing processes and relatively flexible property modification based on a high monomer availability. Therefore, the materials chemistry, physics, manufacturing process techniques, characterization methods, and applications of PIs have been extensively studied [2–17].

In recent years, much attention has been paid to heat-resistant polymers with various photo- and optical functionalities (e.g., photosensitivity [18,19], photoconductivity [20,21],

and electrochromism [22]) while maintaining their intrinsic advantages. Recently, heat-resistant polymers exhibiting electroluminescence (EL) have been extensively investigated for applications in organic light-emitting diode (OLED) image displays and illuminators [23]. Regardless of whether they possess semiconducting properties required for EL applications, heat-resistant polymers with high photoluminescence (PL) functionality are potentially promising for other applications, such as chemical sensors, emission-color conversion devices, fluorescent QR codes, and high-temperature markers.

Highly fluorescent PIs modified with well-designed fluorophores [24–32], fluorescence emission mechanisms [33], brominated PIs exhibiting phosphorescence [34], and emission-wavelength control [35,36] have been investigated. In addition, the pressure effects on the PL properties of PIs have been studied in detail [37]. The difficulty in obtaining highly photoluminescent PIs arises from the charge-transfer (CT) interactions inherent to aromatic PIs [38] and the concentration-quenching (CQ) effect due to prominent fluorophore aggregation in the PI solid films.

So far, we have successfully developed high-performance, optically transparent PIs [39,40]. The approaches used to improve the optical transparency of PI films were based on controlling the CT interactions. This strategy is similar to that for obtaining intense PL functionality. This study presents heat-resistant polymers that emit intense PL in the visible range at room temperature in air [41,42] and discuss the impacts of fluorophore aggregation and CT interactions on the PL properties. The application of a reactive dye as a fluorescence probe is also proposed.

In this study, we used "photoluminescence" as the term representing emission generated by UV-irradiation because we did not separate fluorescence and phosphorescence during the steady-state emission measurements, although this study virtually focused on fluorescence.

2. Experimental Section

2.1. Materials

2.1.1. Synthesis of 9,10-bis(4-aminophenyl)anthracene (BAPA)

BAPA was synthesized according to the procedures described in the literature [43]. In a three-necked flask, a mixture of anthraquinone (1.90 g, 9.12 mmol), anilinium chloride (4.76 g, 36.70 mmol), and aniline (9.3 mL) was refluxed at 185 °C for 3 h in a nitrogen atmosphere, and the resulting black reaction mixture was cooled to room temperature. A mixed solution of acetone (60 mL), methanol (60 mL), and conc. HCl (10 mL) was added to the mixture, and it was stirred in an ice bath for several hours. The precipitate formed was collected by filtration and washed with methanol. Then, this precipitate was added to a mixed solution of acetone (70 mL) and conc. HCl (10 mL) and stirred for 3 h to wash it thoroughly. The precipitate was collected by filtration, washed with acetone, and then neutralized with a NaOH aqueous solution and washed with water. The crude product was dried at 100 °C for 12 h under vacuum (yield: 31%). The green solid obtained was recrystallized from benzene (recrystallization yield: 57%).

The product was characterized as follows. Melting point [differential scanning calorimetry (DSC), heating rate: 5 °C/min]: 323 °C (very sharp endothermic peak). FT-IR (KBr plate method, cm^{-1}): 3436/3357/3217 (NH_2, N–H stretching), 3061/3028 (C_{Ar}–H), 1619 (NH_2, in-plane deformation), 1519 (1,4-phenylene). ^{1}H-NMR (400 MHz, dimethyl sulfoxide (DMSO)-d_6, δ, ppm): 7.72 [d, 4H (relative integrated intensity: 3.96H), J = 9.9 Hz, 1,4,5,8-protons of the anthracene (ANT) unit], 7.37 [d, 4H (4.09H), J = 9.9 Hz, 2,3,6,7-protons of ANT], 7.07 [d, 4H (4.03H), J = 7.7 Hz, 3,3′,5,5′-protons of the aniline (AN) unit], 6.81 (d, 4H (3.91H), J = 8.0 Hz, 2,2′,6,6′-protons of AN], 5.33 [s, 4H(4.00H), NH_2]. Elemental analysis. Anal. calcd (%) for $C_{26}H_{20}N_2$ (360.46): C, 86.64; H, 5.59; N, 7.77. Found: C, 86.65; H, 5.52; N, 7.62. These results confirm that the product is the desired compound (BAPA).

2.1.2. Synthesis of Model Compounds

2,3,6,7-NTDA-based model compound [M(2,3,6,7-NTDA/CHA)]. In a three-necked flask, cyclohexylamine (CHA, 10 mmol) was dissolved in dehydrated *N,N*-dimethylacetamide (DMAc, 10 mL). To this solution, a DMAc solution (10 mL) containing 2,3,6,7-naphthalen-etetracarboxylic dianhydride (2,3,6,7-NTDA, 5 mmol) was added with a syringe, and the reaction mixture was refluxed at 170 °C for 1 h in a nitrogen atmosphere with continuous magnetic stirring and then cooled to room temperature. The precipitate formed was collected by filtration, washed with ethanol and toluene, and dried at 100 °C for 12 h under vacuum (yield: 84%). The white crude product was recrystallized from chloroform in a refrigerator (recrystallization yield: 72%). Melting point (DSC): 451 °C (very sharp endothermic peak). FT-IR (KBr plate method, cm^{-1}): 3040 (C_{Ar}–H stretching), 2948/2857 (C_{Aliph}–H), 1763/1698 (five-membered imide ring, C=O), 1362 (imide, N–C_{Ar}), 752 (imide ring, deformation). ^{1}H-NMR (400 MHz, CDCl$_3$, δ, ppm): 8.49 [s, 4H (4.00H), Ar-H], 4.25–4.19 [m, 2H (1.91 H), N-CH], 2.28–2.23 [m, 4H (4.04H), N-CH-CH$_{eq}$], 1.92–1.36 [m, 16H (15.6H), the remaining protons of the cyclohexyl (CHX) groups].

1,4,5,8-NTDA-based model compound [M(1,4,5,8-NTDA/CHA)]. An isomer of M(2,3,6,7-NTDA/CHA), M(1,4,5,8-NTDA/CHA), was synthesized using 1,4,5,8-NTDA and CHA in a manner similar to that mentioned above (yield: 88%) and recrystallized from toluene in a refrigerator (recrystallization yield: 82%). Melting point (DSC): 363 °C (very sharp endothermic peak). FT-IR (KBr plate method, cm^{-1}): 2976/2932/2917/2855 (C_{Aliph}–H), 1715/1653 (six-membered imide ring, C=O), 1341 (imide, N–C_{Ar}), 766 (imide ring, deformation). ^{1}H-NMR (400 MHz, CDCl$_3$, δ, ppm): 8.70 [s, 4H (4.00H), Ar-H], 5.05–4.99 (m, 2H (1.96 H), N-CH], 2.55–2.48 [m, 4H (4.05H), N-CH-CH$_{eq}$], 1.93–1.35 [m, 16H, the remaining protons of CHX].

2.1.3. Common Monomers and Conjugated Monofunctional Compounds

The abbreviations, sources, drying or purification conditions, and melting points of the common monomers and conjugated monofunctional compounds used for the polymerization of the polybenzoxazoles (PBOs), polyazomethines (PAzMs), and PI precursors are summarized in Supplementary Materials Tables S1 and S2.

2.1.4. Polycondensation of PBOs via the One-Pot Process and Film Preparation

PBOs were polycondensed via the one-pot process using polyphosphoric acid (PPA) [44]. A typical procedure is as follows: bis(*o*-aminophenol) (5 mmol), dicarboxylic acid (5 mmol), and PPA (115% as H3PO4 equivalent, Sigma-Aldrich Japan, Tokyo, Japan) were placed in a three-necked separable flask, equipped with a mechanical stirrer and nitrogen inlet/outlet. The initial solid content was ~10 wt%. The reaction mixture was gradually heated to 200 °C in a nitrogen atmosphere with continuous mechanical stirring and held at this temperature for 2 h. Afterwards, the reaction mixture was gradually poured into a large quantity of water, and the resulting fibrous precipitate was repeatedly washed with water and methanol and dried at 100 °C for 24 h under vacuum.

The formation of PBOs was confirmed by transmission-mode FT-IR spectroscopy (Jasco, Tokyo, Japan, FT/IR 4100 infrared spectrometer) using separately prepared thin films. As a typical example, the following specific infrared bands (cm^{-1}) were observed for the 6FAP/1,3-CHDCA system: 2942/2865 (C_{Aliph}–H stretching), 1620 (oxazole ring, C=N), 1202 (CF$_3$, C–F), 963 (CF$_3$–C–CF$_3$, C–C). In addition, the unnecessary infrared bands characteristic to the PBO precursor (polyhydroxyamide) (amide, C=O stretching band at 1655/1537 cm^{-1}) and residual 1,3-CHDCA monomer (hydrogen-bonded COOH, O–H stretching band at ~2600 cm^{-1} and C=O stretching band at ~1700 cm^{-1}) were not observed. The results indicate the formation of PBO.

The PBO fibrous powder was dissolved in anhydrous *N*-methyl-2-pyrrolidone (NMP) at a solid content of ~10 wt%, and the resulting homogeneous solution was coated on a glass substrate and dried at 80 °C for 2 h in an air-convection oven and subsequently heated

at 200 °C for 1 h on the substrate under vacuum. The PBO films formed (typically 20 μm thick) were then annealed at 220 °C (or 250 °C) for 1 h under vacuum without the substrate.

2.1.5. Polycondensation of PAzMs and Film Preparation

Terephthalaldehyde (TPAL) (4.95 mmol) and conjugated monoaldehyde (0.1 mmol) were added to an *m*-cresol solution of 2,2-bis[4-(4-aminophenoxy)phenyl]hexafluoropropane (HFAPP, 5 mmol) with an initial solid content of 36 wt%. The reaction mixture was stirred at room temperature for 24 h, during which the mixture was gradually diluted with a minimal quantity of *m*-cresol to avoid precipitation. After the reaction, a homogeneous polyazomethine (PAzM) solution was gradually poured into a large quantity of methanol, and the precipitate formed was collected by filtration, washed with methanol, and dried at 100 °C for 24 h under vacuum.

The formation of PAzM was confirmed by FT-IR spectroscopy using separately prepared thin films. The following specific infrared bands (cm^{-1}) were observed: 3050 (C_{Ar}–H stretching), 2878 (N=CH, C_{Aliph}–H), 1625/1613 (C=N), 1495 (1,4-phenylene), 1250 (C_{Ar}–O–C_{Ar}). In addition, the unnecessary infrared bands characteristic to residual HF-BAPP monomer (e.g., NH_2, N–H stretching bands at 3400–3200 cm^{-1}) were not observed. These results indicate the formation of PAzM.

The isolated fibrous powder was re-dissolved in fresh NMP. The homogeneous solution formed was coated on a glass substrate and dried at 150 °C for 1 h in an air-convection oven. The resulting PAzM film was subsequently annealed at 250 °C for 1 h under vacuum without the substrate.

2.1.6. Polyaddition of PI Precursors [Poly(amic acid) (PAA)], Imidization, and Film Preparation

In all the PI systems using cycloaliphatic diamines [typically, 4,4′-methylenebis(cyclohexylamine (MBCHA)], PI films were prepared via the two-step process. A typical procedure is as follows. First, tetracarboxylic dianhydride (TCDA) powder (5 mmol) was added in several portions to a DMAc solution of diamine (5 mmol) with continuous magnetic stirring at room temperature, and the reaction mixture with an initial solid content of 15 wt% was stirred for 24–72 h in a sealed bottle until it became homogeneous and reached a maximal solution viscosity. During the polyaddition, the reaction mixture was gradually diluted as appropriate with the minimal quantity of the same solvent needed to ensure effective stirring. If the conjugated diamines used were poorly soluble in DMAc at room temperature (typically, *N*,*N*′-disubstituted 3,4,9,10-perylenetetracarboxylic diimide-based diamines), they were pre-dissolved in DMAc by lightly heating for a very short time in a test tube and then promptly cooled to room temperature for use in the polyaddition.

The formation of PAAs was confirmed by FT-IR spectroscopy using separately prepared thin films. As a typical example, the following specific infrared bands (cm^{-1}) were observed for the 2,3,6,7-NTDA/MBCHA system: 3279 (amide, N–H stretching), 3077 (C_{Ar}–H), 2928/2855 (C_{Aliph}–H), 2502 (hydrogen-bonded COOH, O–H), 1713 (COOH, C=O), 1628/1549 (amide, C=O). In addition, the unnecessary infrared bands due to residual 2,3,6,7-NTDA monomer (e.g., acid anhydride, C=O stretching band at ~1850 cm^{-1}) were not observed. The results indicate the formation of PAA.

The resultant homogeneous PAA solution was diluted as appropriate, bar-coated on a glass substrate, and then dried at 60 °C (or 80 °C for NMP) for 2 h in an air-convection oven. The resulting PAA film was thermally imidized at 200 °C for 1 h + 300 °C for 1 h on the substrate under vacuum. Subsequently, the film was annealed at 320 °C for 1 h under vacuum without the substrate to remove residual stress for the subsequent thermo-mechanical analysis. In some cases, the thermal conditions during the film preparation were optimized by fine tuning to obtain a better quality of PI films.

The progress of thermal cyclodehydration (imidization) was confirmed by FT-IR spectroscopy using separately prepared thin films. As a typical example, the following specific infrared bands (cm^{-1}) were observed for the 2,3,6,7-NTDA/MBCHA system:

2926/2853 (C_{Aliph}–H stretching), 1767/1711 (imide, C=O), 1354 (imide, *N*–C_{Aliph}), and 752 (imide ring, deformation). In addition, the unnecessary infrared bands characteristic to the PAA (amide, C=O stretching bands at 1628/1549 cm^{-1}) completely disappeared. The results indicate that thermal imidization was completed.

In a selected system, chemical imidization was conducted by gradually adding a cyclodehydration agent [acetic anhydride (Ac_2O)/pyridine (10/3, *v/v*)] to the PAA solutions with a fixed molar ratio of $[Ac_2O]/[COOH]_{PAA} = 5$ and stirring for 12 h at room temperature in a sealed bottle. The resultant homogeneous reaction mixture was diluted as appropriate with the same solvents and gradually poured into a large quantity of methanol. The fibrous precipitate obtained was filtered off and dried at 100 °C for 12 h under vacuum.

The progress of chemical imidization was confirmed by FT-IR spectroscopy using separately prepared thin films. The following specific infrared bands (cm^{-1}) were observed for the HTA-44BP/TFMB-based system: 3042 (C_{Ar}–H stretching), 2948/2868 (C_{Aliph}–H), 1752 (imide, C=O), 1721 (imide, C=O + ester, C=O), 1493 (1,4-phenylene), 1375 (imide, *N*–C_{Ar}), and 1314/1171 (CF_3, C–F). In addition, the unnecessary infrared bands characteristic to the PAA (amide, C=O stretching bands at ~1660/1540 cm^{-1}) completely disappeared. The results indicate that chemical imidization was completed.

The chemically imidized powder sample was dissolved in a fresh anhydrous solvent. The resulting homogeneous PI solution was coated on a glass substrate and dried at 80 °C for 2 h in an air-convection oven, and subsequently heated at 200 °C for 1 h on the substrate. The resulting PI films (typically 20 μm thick) were then annealed at a temperature 10–20 °C lower than the T_g for 1 h under vacuum without the substrate.

In this study, the chemical compositions of the PI and PBO systems are abbreviated using the symbols of their monomer components as "X/Y" for homo PIs, "X1;X2/Y1;Y2" for copolyimides (X: TCDAs, Y: diamines), and "A/B" for homo PBOs [A: bis(*o*-aminophenol)s, B: dicarboxylic acids].

2.2. Measurements

2.2.1. Ultraviolet (UV)–Visible Absorption Spectra

The UV-visible absorption spectra of the monomers and model compounds in solutions and the PI and PBO films were measured at room temperature in the wavelength (λ) range of 200–800 nm with a bandpass of 0.5 nm using a UV-visible spectrophotometer (Jasco, Tokyo, Japan, V-530).

2.2.2. Photoluminescence (PL) Spectra and PL Quantum Yields

The photoluminescence (PL) spectra of the monomers and model compounds in solutions were measured at room temperature in a fluorescence-free quartz cell at an ordinary right-angle arrangement using a fluorescence spectrometer (Hitachi, Tokyo, Japan, F-4500). The PL spectra of the film specimens, sandwiched between fluorescence-free quartz plates and mounted on a film sample holder (Hitachi 650-0161), were measured in a front-face reflection geometry at room temperature. An adequate sharp-cut filter, which does not deform the spectra, was selected and placed in front of the emission-side monochromator to remove unnecessary scattered light. The bandpass of the emission- and excitation-side monochromators was set at 5 nm, respectively. The excitation spectra in the range of 200–600 nm were corrected for the λ-dependence of the light intensity from the Xe lamp using a rhodamine B screen solution (Wako Chemical, Osaka, Japan) in a triangular quartz cell (Hitachi 650-1640). The PL spectra in the range of 200–600 nm were corrected for the λ-dependent detector sensitivity using a light diffuser (Hitachi 650-1576) by simultaneously sweeping the wavelengths of the excitation and emission monochromators. A sub-standard tungsten light source (Hitachi 250-0123) was also used for the spectral correction in a longer wavelength range (500–900 nm). These procedures allowed for PL spectrum corrections in the range of 200–900 nm.

The PL quantum yields (Φ_{PL}) of the solution samples were determined by the following relationship:

$$\Phi_{PL}/\Phi_{PLst} = [(I_f/A)/(I_{f\,st}/A_{st})] \times (n^2/n_{st}{}^2) \tag{1}$$

where I_f and $I_{f\,st}$ denote the integrated PL intensities of the sample and standard solutions; A and A_{st}, adjusted to an adequate value (0.05–0.1), represent the absorbance of the sample and standard solutions at the excitation wavelength (λ_{EX}); and n and n_{st} are the average refractive indices of the solvents for the sample and standard solutions, respectively. A 1 N-sulfuric acid aqueous solution of quinine sulfate dihydrate was used as the standard solution with a known Φ_{PL} value ($\Phi_{PL\,st}$ = 0.55 [45]).

The Φ_{PL} values of the film samples were estimated from the following relationship:

$$\Phi_{PL}/\Phi_{PL\,st} = \{I_f/[1 - \exp(-2.303A)]\}/\{I_{f\,st}/[1 - \exp(-2.303A_{st})]\} \tag{2}$$

In this case, a dye-dispersed poly(methyl methacrylate) (PMMA) film was prepared as the standard film sample as follows. First, *N,N′*-bis(2,4-di-*tert*-butylphenyl)perylene-3,4,9,10-tetracarboxydiimide (DBu-PEDI; Sigma-Aldrich Japan, Tokyo, Japan), which exhibits an extremely high Φ_{PL} value close to unity in chloroform (Φ_{PL} = 0.95) [46], and PMMA pellets (Wako Chemical, Osaka, Japan) were separately dissolved in chloroform, and these solutions were mixed with an established ratio. The mixed solution was coated on a glass plate and dried at 60 °C for 1 h in an air-convection oven. The DBu-PEDI concentration in the cast films was adjusted to 1.0×10^{-4} mol/L to avoid dye aggregation and spectral deformation due to self-reabsorption. The DBu-PEDI-dispersed PMMA solid film exhibited virtually the same normalized I_f value as that of its poly(vinyl chloride) (PVC) counterpart. This suggests that the PMMA film is similarly regarded as an inert matrix, as well as the film of PVC with a similar structure to chloroform. Therefore, the Φ_{PL} of the DBu-PEDI-dispersed PMMA film was reasonably assumed to be virtually equivalent to that of the chloroform solution (Φ_{PL} = 0.95).

2.2.3. PL Image

The film specimens were photographed in the dark while irradiating the upper face of the films at an adequate tilt angle using a broadband UV lamp (Topcon, Tokyo, Japan, PUV-1A) with a continuous spectral distribution over the range of 250–405 nm.

2.2.4. Reduced Viscosities

The reduced viscosities (η_{red}) of the PAAs (and/or PIs for soluble systems) and PBOs, which can be regarded as being equivalent to the inherent viscosities (η_{inh}), were measured at 30 °C in the same solvents as those used in the polymerization at a solid content of 0.5 wt% using an Ostwald viscometer.

2.2.5. Linear Coefficients of Thermal Expansion (CTE)

The CTE values of the film specimens (15 mm long, 5 mm wide, and typically 20 μm thick) in the X–Y direction below their T_gs were measured by thermomechanical analysis (TMA) as averages in the range of 100–200 °C at a heating rate of 5 °C min^{-1} using a thermomechanical analyzer (Netzsch Japan, Yokohama, Japan, TMA 4000) with a fixed load (0.5 g static load per 1 μm thickness, i.e., 10 g load for 20 μm thick films) in a dry nitrogen atmosphere. In this case, after the preliminary first heating run up to 120 °C and subsequent cooling to room temperature in the TMA chamber, the data were collected from the second heating run to remove any influence of adsorbed water.

2.2.6. Heat Resistance

The glass transition temperatures (T_gs) of the PI and PBO films were determined from the peak temperature of the loss energy (E'') curves by dynamic mechanical analysis (DMA) at a heating rate of 5 °C min^{-1} on the TMA instrument (as before). The measurements

were conducted at a sinusoidal load frequency of 0.1 Hz with an amplitude of 15 gf in a nitrogen atmosphere.

The thermal and thermo-oxidative stability of the PI and PBO films were evaluated from the 5% weight loss temperatures ($T_d{}^5$) by thermogravimetric analysis (TGA) on a thermo-balance (Netzsch Japan, Yokohama, Japan, TG-DTA2000). TGA was performed by heating the sample-charged open aluminum pan from 30 to 500 °C at a heating rate of 10 °C min^{-1} in a dry nitrogen and/or air atmosphere. A small weight loss due to desorbed water around 100 °C during the TGA heating runs was compensated for the data analysis by implementing an offset at 150 °C to 0% weight loss.

2.3. Model Reaction of Transamidation in PAA Solutions

An equimolar polyaddition of 3,3′,4,4′-biphenyltetracarboxylic dianhydride (*s*-BPDA) and *p*-phenylenediamine was conducted in DMAc at a solid content of 10 wt% at room temperature, and a homogeneous, viscous solution of PAA (η_{red} = 3.84 dL/g) was obtained. To this PAA solution (9 mL), a DMAc solution (0.5 mL) of *N*,*N*′-bis[4-(4-amino-3-methylbenzyl)-2-methylphenyl]-3,4,9,10-perylenetetracarboxydiimide (PEDI-MBMA) with a concentration of 6.56 × 10^{-3} M was added, and the mixture was vigorously stirred in a sealed bottle. The vessel was set in a deflated, heat-sealed polyethylene bag and soaked in a water bath regulated at 20 °C. A small quantity of the mixed solution (0.12 g) was sampled at each storage time and promptly diluted with dry DMAc to an adequate concentration for the subsequent prompt PL measurements. For comparison, the mixed solution of the methyl ester of the PAA [i.e., poly(amide methyl ester), PAE] and PEDI-MBMA was also prepared in a similar manner.

3. Results and Discussion

### 3.1. PL and Thermal Properties of Heat-Resistant Polymers

3.1.1. Polybenzoxazoles

We previously developed optically transparent PBOs using the one-pot process in PPA at elevated temperatures [47]. In this study, as an extension of our previous research, the PL properties of PBO systems (Figure 1) were investigated. Table 1 summarizes their thermal and PL properties. The use of cycloaliphatic dicarboxylic acids [1,3-cyclohexanedicarboxylic acid (1,3-CHDCA) and 1,4-CHDCA] or fluorinated aromatic dicarboxylic acid [2,2-bis(4-aminophenyl)hexafluoropropane (Bis-B-AF)] afforded soluble PBOs in various solvents. In particular, the Bis-B-AF-based PBO films exhibited a very high T_g exceeding 300 °C. Their T_g values increased with an increase in the structural rigidity of the bis(*o*-aminophenol)-based bisbenzoxazole units in the following order: ADPE (#4, T_g = 298 °C) < 6FAP (#7, 320 °C) < *p*-HAB-based system (#2, 340 °C). In addition, as expected, the use of aromatic dicarboxylic acids (OBA and Bis-B-AF) afforded PBO films with a much higher thermal stability [$T_d{}^5$ (N$_2$)] and thermo-oxidative stability [$T_d{}^5$ (air)] than those of the counterparts from cycloaliphatic dicarboxylic acids. None of the PBO systems listed in Table 1 showed low CTEs, reflecting their distorted (non-linear) main chain structures. Among them, the wholly aromatic PBO film obtained using *p*-HAB with a rigid structure and aromatic Bis-B-AF exhibited a somewhat reduced CTE (40.0 ppm/K).

The combinations of aromatic bis(*o*-aminophenol)s with aromatic dicarboxylic acids are expected to generate intense PL because the resultant PBOs contain in common a 2-phenylbenzoxazole (2-PhBO) structural unit in their main chains, which shows extremely intense fluorescence owing to the electronic conjugation between the 2-phenyl group and the benzoxazole (BO) unit [Φ_{PL} = 0.75 (75%) in *n*-heptane at room temperature [48]]. However, contrary to this prediction, the *p*-HAB/Bis-B-AF PBO film (#2), as well as the ADPE/Bis-B-AF film (#4), did not show intense PL. The results are likely ascribed to close stacking between the 2-PhBO units and, concomitantly, the CQ effect. On the other hand, PL was clearly enhanced in the 6FAP/OBA system (#8). This can be interpreted as the result of somewhat disrupted stacking (CQ effect) owing to the bulky hexafluoroisopropylidene (HFIP) side groups originating from 6FAP, explaining why the wholly aromatic PBO films

(#2 and #4) did not exhibit intense PL. Furthermore, the 6FAP/Bis-B-AF system (#7), including the HFIP side groups in both monomers (6FAP and Bis-B-AF), exhibited a significantly enhanced PL spectrum with Φ_{PL} = 0.22 (22%), as shown in Figure 2. This result is also consistent with the afore-mentioned hypothesis. By contrast, the semi-aromatic 6FAP/1,4-CHDCA system (#9) showed a PL spectrum in the UV range. Thus, the combination of the conjugated 2-PhBO units with the stacking-disturbing bulky side groups (typically, HFIP groups) was indispensable for generating intense, visible PL from the PBO films.

In this study, a conjugated monomer, i.e., 3,9-perylenedicarboxylic acid (3,9-PEDCA), was used as a comonomer to modify PBOs. Owing to its poor solubility, a small amount of 3,9-PEDCA (1 mol%) was incorporated into the 6FAP/OBA system. The modified PBO film (#10) exhibited a relatively intense, green PL spectrum (Φ_{PL} = 0.26) with an emission peak wavelength (λ_{EM}) at 515 nm (Figure 3).
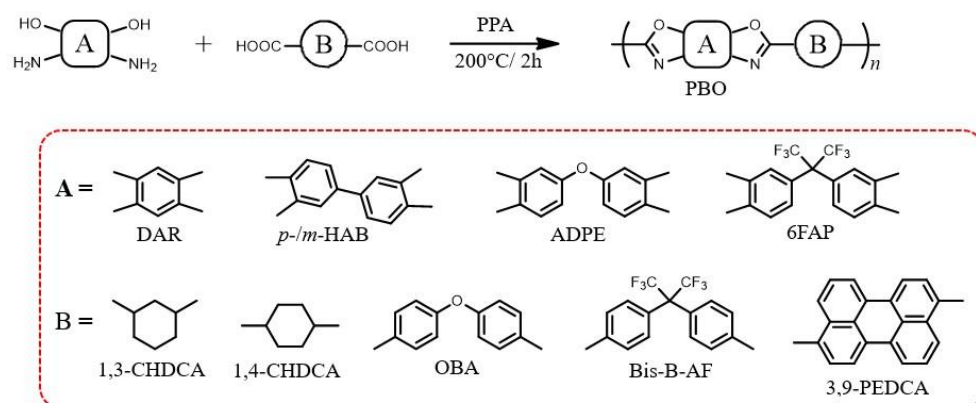

Figure 1. Structures of polybenzoxazole (PBO) films prepared via one-pot polycondensation.

Table 1. Structures, photoluminescence (PL), and thermal properties of polybenzoxazole (PBO) films prepared via one-pot polycondensation.

No.	Bis(*o*-aminophenol) (mol%)	Dicarboxylic Acid (mol%)	η_{red} (dL/g)	T_g (°C)	T_d^5 (N$_2$) (°C)	T_d^5 (Air) (°C)	CTE (ppm/K)	Abs at λ_{EX}	λ_{EX} (nm)	λ_{EM} (Peak) (nm)	Φ_{PL}
1	DAR	1,3-CHDCA [a]	2.17	325			48.0	0.36	350	391	0.026
2	*p*-HAB	Bis-B-AF	1.51	340	529	524	40.0	>3	350	427	0.011
3	*m*-HAB	1,3-CHDCA [a]	2.33	241			51.1	0.30	350	424	0.017
4	ADPE	Bis-B-AF	1.46	298	528	517	57.0	1.78	370	420	0.013
5		1,3-CHDCA [a]	1.30	195	470	443	55.3	>3	310	363/477	0.015
6		1,4-CHDCA [a]	6.08	217	486	418	68.1	>3	310	367/558	0.0032
7	6FAP	Bis-B-AF	0.56	320	513	510	55.0	0.66	350	404/428	0.22
8		OBA	0.89	302	533	522	51.0	0.32	350	387/409	0.065
9		1,4-CHDCA [a]	2.16	269	483	377	64.5	0.25	325	365/380	0.14
10		OBA (99) 3,9-PEDCA (1)	0.39	291	530	520	55.7	1.08	469	515	0.26

[a] The thermal properties were cited from ref. [47].
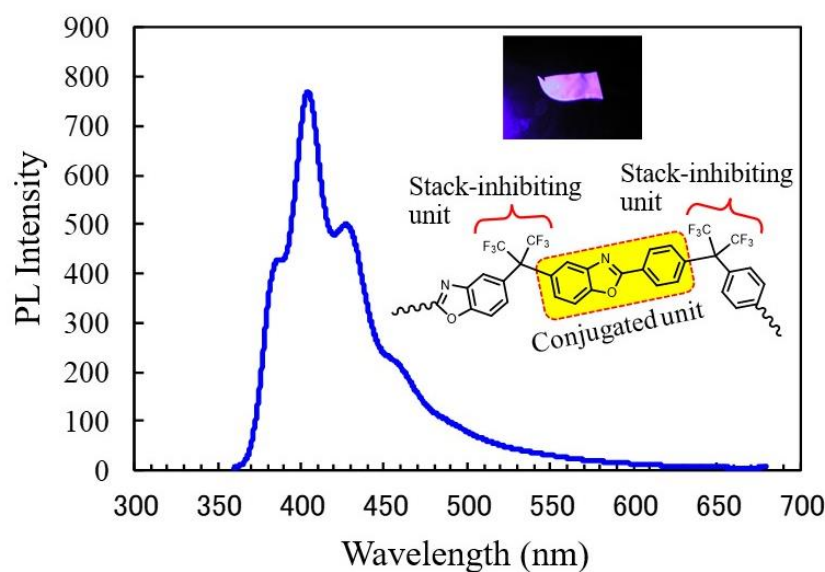
Figure 2. Photoluminescence (PL) spectrum of the PBO film prepared using 6FAP and Bis-B-AF (#7) via the one-pot polycondensation process. Inset: PL image of the PBO film.
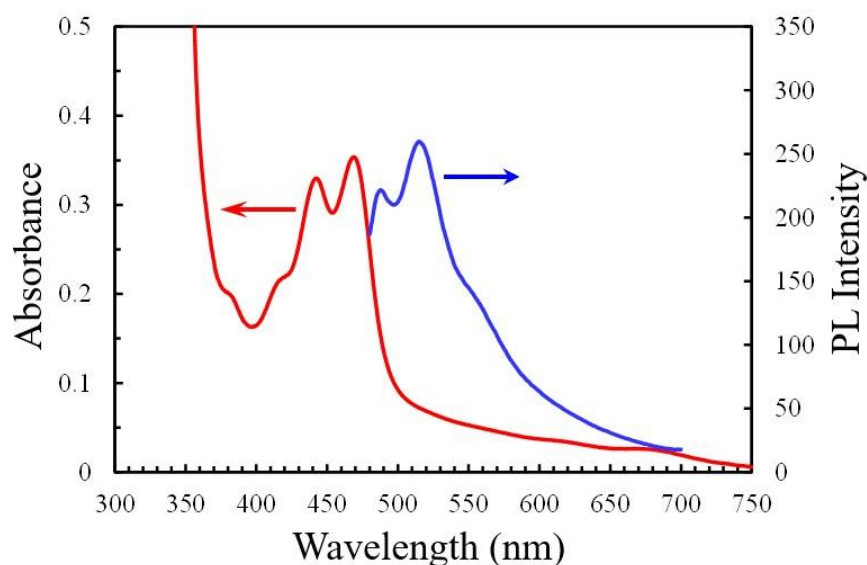

Figure 3. UV-visible absorption (red curves) and PL spectra (blue curves) of the PBO film prepared using 6FAP with OBA (99 mol%) and 3,9-PEDCA (1 mol%) via one-pot polycondensation.

3.1.2. Terminal-Modified Polyimides with Conjugated Monoamines

As a simple approach used to impart intense and visible PL functionality to PIs, their terminal modification using conjugated monoamines, which is likely effective in avoiding CQ, can be applied. Terminal-modified PI films were prepared according to the schemes shown in Figure 4. To ensure preferential light absorption of the terminal fluorophores, wholly cycloaliphatic PIs were selected as their backbone structures because they maintain high light transmittance in the UV range (cut-off wavelength: 260 nm). In the initial stage of the polyaddition of cycloaliphatic diamines and TCDAs, an insoluble salt is formed owing to the high basicity of the aliphatic diamines; this often disturbs the smooth progress of polyaddition [39]. In this study, the combination of 1,2,3,4-cyclobutanetetracarboxylic dianhydride (CBDA) and MBCHA was selected as a host polymer because a homogeneous and viscous solution of high-molecular-weight PAA can finally be obtained by prolonged stirring at room temperature with the gradual dissolution of the initially formed salt. The resultant PAA provided a flexible PI film via thermal imidization. In this study, the

monoamine content was controlled at 1 mol% to avoid serious film embrittlement due to a significant decrease in their molecular weights.
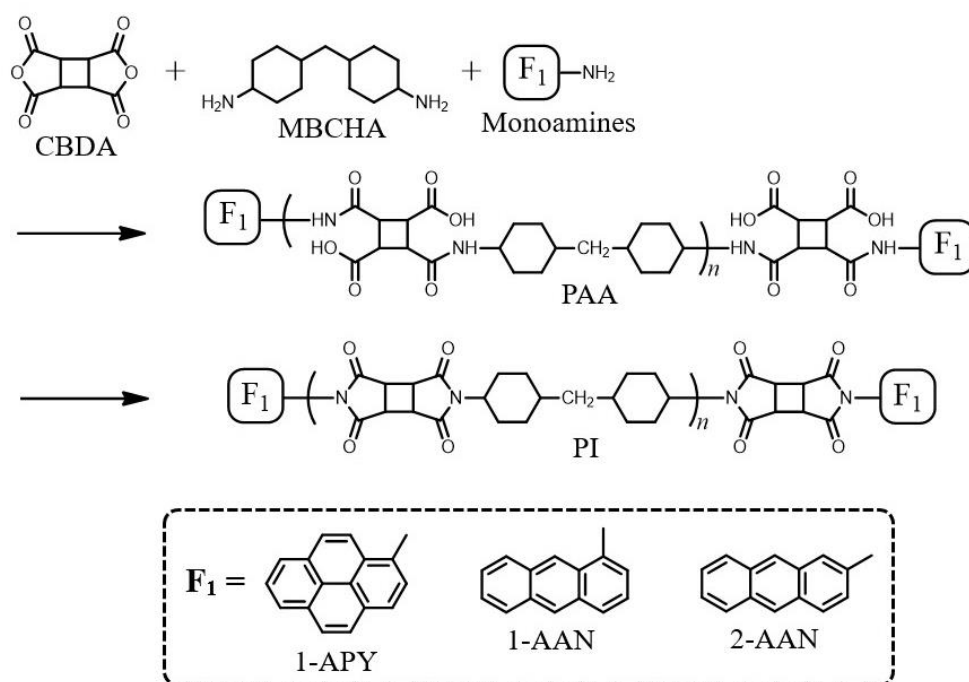
Figure 4. Structures of wholly cycloaliphatic polyimides (PIs) containing terminal conjugated aromatic groups.

The thermal and PL properties of the terminal-modified PI films are summarized in Table 2. The PI films showed very high T_g values in the range of 327–334 °C and a relatively high thermal stability [T_d^5 (N$_2$) = 424–432 °C] with decreased T_d^5 (air) values (367–378 °C) based on their non-aromatic structures. These films did not exhibit preferable low CTE characteristics (62.4–66.0 ppm/K) owing to their non-linear main chain structures originating from MBCHA. These CBDA/MBCHA-based PIs were essentially insoluble in common solvents. Therefore, the chemical imidization and one-pot processes were not applicable.

Table 2. PL and thermal properties of CBDA-based wholly cycloaliphatic polyimides (PIs) containing terminal conjugated aromatic groups.

No.	Diamine (mol%) Monoamine (mol%)	η_{red} (PAA) (dL/g)	T_g (°C)	T_d^5 (N$_2$) (°C)	T_d^5 (Air) (°C)	CTE (ppm/K)	λ_{EX} (nm)	λ_{EM} (Peak) (nm)	Φ_{PL}
11	MBCHA (99.5) 1-APY (1.0)	1.16	334	429	372	66.0	330	375, 394	0.26
12	MBCHA (99.5) 1-AAN (1.0)	0.820	334	429	373	63.9	365	392, 413, 438	0.12
13	MBCHA (99.5) 2-AAN (1.0)	0.704	330	424	367	62.4	343	387, 408, 441, 470	0.12

1-Aminopyrene (1-APY) showed a considerably intense, structureless PL spectrum (λ_{EX} = 360 nm) with a peak at 429 nm in ethanol, as shown in Figure 5a. This spectral shape without vibronic structures was quite different from that of the non-substituted pyrene, whose spectrum shows a fine vibronic structure [49]. The disappearance of the vibronic structure in the PL spectrum of 1-APY in solution probably results from the internal rotation of the amino group during its excited-state lifetime, which creates numerous conjugated states between the amino group and the pyrene unit. By contrast, in the terminal-modified PI film with 1-APY, an intense PL spectrum (Φ_{PL} = 0.26) with a distinct vibronic structure

(such as pyrene) was observed, as shown in Figure 5b. The significant PL spectral change [from structureless (a) to structured (b)] reflects that 1-APY is covalently bound to the PI chain ends. The recovered vibronic structure is ascribed to the conversion of the amino group to the electron-withdrawing imide group, by which the conjugation between the amino group and pyrene unit is significantly reduced. In addition, a clear mirror image, which provides useful photophysical information, as discussed later, was observed between the UV-visible absorption and the PL spectra (Figure 5b).
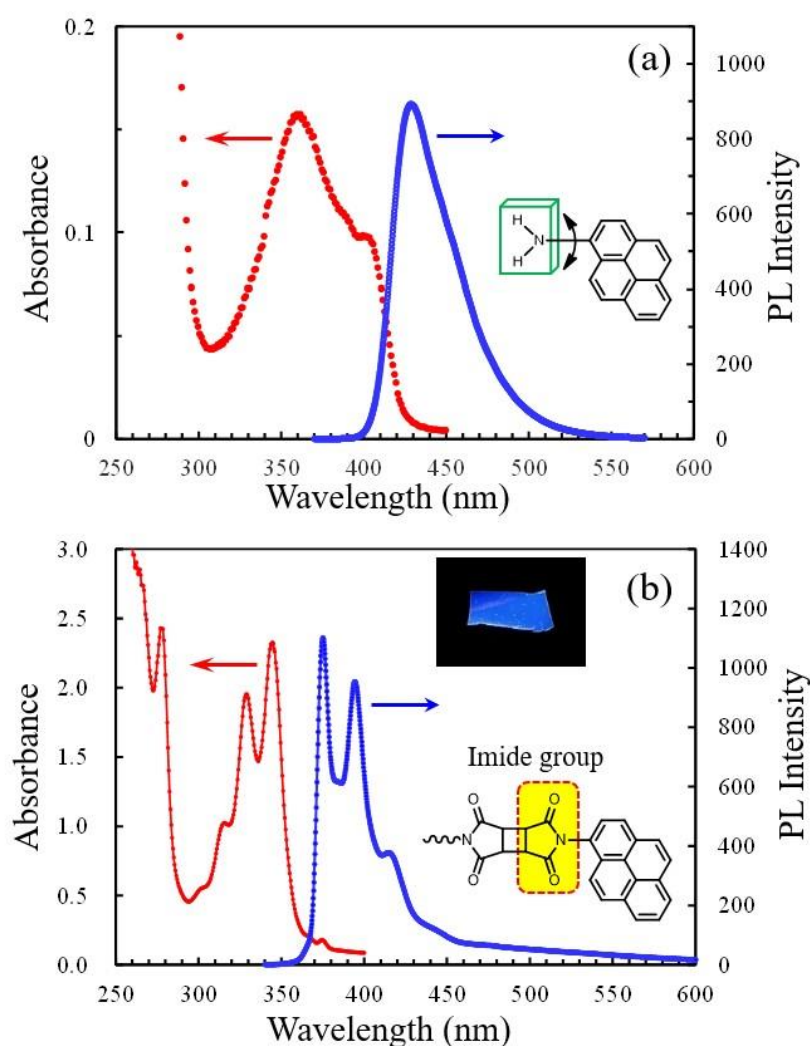
Figure 5. UV-visible absorption (red curves) and PL spectra (blue curves) of 1-APY in ethanol (1.0×10^{-5} mol/L, λ_{EX} = 360 nm) (**a**) and 1-APY-terminated CBDA/MBCHA-based PI film (**b**). Inset: PL image of the PI film.

A similar behavior in the PL spectra (disappearance and recovery of the vibronic structure and the appearance of mirror image) was also observed in 1- and 2-aminoanthracene (AAN) in solution and the corresponding terminal-modified PIs. These PI films exhibited relatively intense blue PL spectra with Φ_{PL} = 0.12 (Table 2).

### 3.1.3. Terminal-Modified Polyazomethines with Conjugated Monoaldehydes

The afore-mentioned terminal-modified PIs do not have semiconducting properties because they are primarily composed of cycloaliphatic structures; therefore, they cannot serve as the emitting layer in EL devices. In contrast, PAzM is a heat-resistant conjugated polymer. However, PAzMs are generally non-photoluminescent [50]. If PAzMs are endowed with intense PL functionality, they can become useful materials for EL applications.

A pronounced PL enhancement effect of intramolecular hydrogen bonds [51] and coordination bonds [52], which can contribute to disturbing E/Z photo-isomerization in the C=N units, has been reported.

We attempted to give PL functionality to PAzMs via terminal modification with conjugated monoaldehydes according to the reaction scheme shown in Supplementary Materials Figure S1. The PAzM system, derived from terephthalaldehyde (TPAL) and 2,2-bis[4-(4-aminophenoxy)phenyl]hexafluoropropane (HFBAPP), was selected as the main backbone structure because it had solution-processability for film preparation. The non-modified, original PAzM film possessed a T_g of 205 °C and a $T_d{}^5$ (N$_2$) of 458 °C [53], which are much higher than those of common polymers. PAzMs and PBOs contain a similar structure, i.e., the Ar-N=C-Ar′ unit, although, strictly speaking, the Ar-N=C-Ar′ unit of the former consists of a distorted *trans*-form [54], and that of the latter adopts a coplanar *cis*-form. The terminal-modified PAzM with 1-pyrenealdehyde (1-PYAL), as well as that modified with 9-anthracenealdehyde (9-AAL), remained non-photoluminescent. There is a possibility that the excitation energy was effectively consumed by E/Z isomerization in the Ar-N=C-Ar′ unit. Thus, our attempt to obtain PAzMs with high PL functionality using this terminal modification method was unsuccessful.

3.1.4. Polyimides Derived from Common Aromatic Tetracarboxylic Dianhydrides with Cycloaliphatic Diamines

So far, we have investigated the PL properties of PIs obtained using conjugated monomers [41,42]. Prior to describing these results, in order to discuss the influence of the extent of conjugation in the tetracaboxydiimide (TCDI) local structures on the PL properties later, we briefly review the PL properties of PIs derived from common aromatic TCDAs (PMDA, *s*-BPDA, etc.; Figure 6) and cycloaliphatic diamines, some of which have been reported previously. In these systems, the aromatic TCDI units as fluorophores are "intramolecularly" isolated by alternately connected "inert" cycloaliphatic units. Thus, "intramolecular" CQ or another fluorescence-quenching mechanism (e.g., via photo-induced electron transfer (PIET)] can be excluded in these systems.
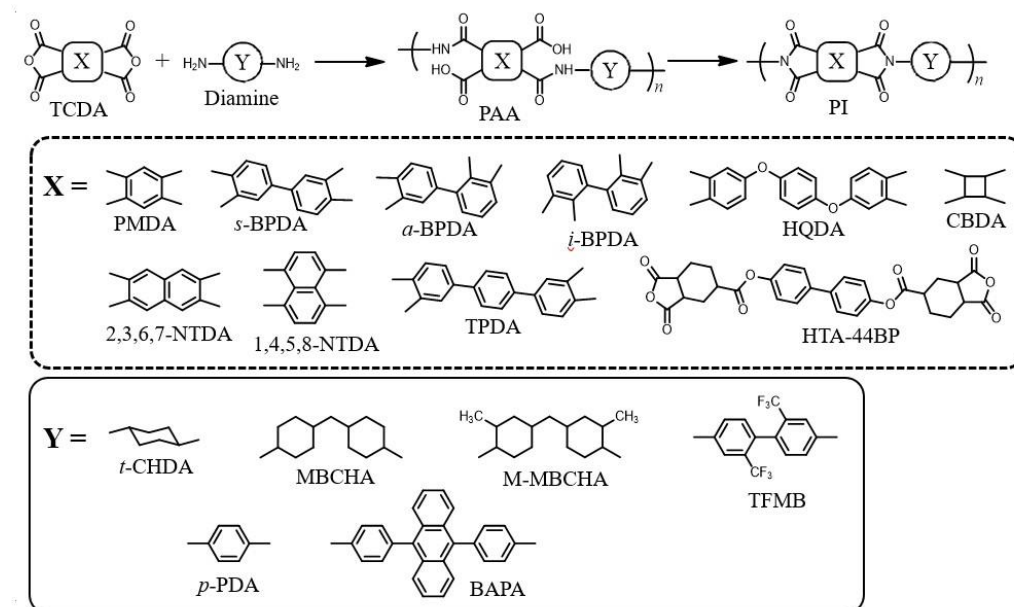
Figure 6. Structures of the PAAs, PIs, and monomers used in this study [tetracarboxylic dianhydrides (TCDAs, X) and diamines (Y)].

The thermal and PL properties of these systems are summarized in Table 3. The PMDA/MBCHA system (#14) provided a colorless and clear (hazeless) PI film with the highest T_g (342 °C) among those listed in this table. However, this PI film did not have prominent PL functionality; the PL was weak, with a peak at 430 nm.

Table 3. PL and thermal properties of PIs derived from common aromatic tetracarboxylic dianhydrides with cycloaliphatic or aromatic diamines.

No.	Tetracarboxylic Dianhydride	Diamine	η_{red} (PAA) (dL/g)	T_g (°C)	T_d^5 (N$_2$) (°C)	T_d^5 (Air) (°C)	CTE (ppm/K)	λ_{EX} (nm)	λ_{EM} (Peak) (nm)	Φ_{PL}
14	PMDA	MBCHA	1.44	342	464	390	55.0	300	430	0.0019
15		M-MBCHA	1.17	307	436	360	59.0	300	435	0.0016
16		*t*-CHDA	1.55	360	481	444	9.5	300	405	0.080
17		MBCHA	1.21	232	470	442	62.3	300	414	0.050
18	*s*-BPDA	M-MBCHA	1.00	253	438	365	53.0	300	406	0.024
19		TFMB	1.65	310	>550	>550	34.8	300	479 (CT)	0.013
20		*p*-PDA	1.78	370	587	571	10.3	300	537 (CT)	0.0021
21	*a*-BPDA	MBCHA	0.623	289	465	426	56.1	300	396	0.0012
22	*i*-BPDA	MBCHA	0.281	-[a]	-[a]	-[a]	-[a]	300	394	0.0078
23	HQDA	MBCHA	1.50	217	-	-	75.3	350	434	0.061 (0.11)[b]
24	CBDA (90) HQDA (10)	MBCHA	0.78	346	435	386	63.8	350	424	0.064 (0.067)[c]
25	TA-HQ	MBCHA[d]	2.41	ND[e]	437	376	51.5	350	465	0.0016
26	TA-44BP	MBCHA	0.49	212	447	396	62.4	350	530	0.0019

[a] The thermal properties were not measured because the film was broken into small pieces. [b] Data cited from ref. [33]. [c] Data for the CBDA(98); HQDA(2)/MBCHA copolymer film. [d] MBCHA re-crystallized from cyclohexane was used. [e] ND: Not detected by DMA.

The effect of the cycloaliphatic diamine structure on the PL yield was also investigated in this study. The use of methyl-substituted MBCHA [4,4′-methylenebis(2-methylcyclohexylamine), M-MBCHA, #15], which is expected to be more effective than its non-substituted counterpart (MBCHA) in disturbing close stacking between the pyromellitdimide (PMDI) units, resulted in no distinct PL enhancement. The results suggest that the weak PL character of the PMDA/MBCHA film probably originates from an inherent character of the PMDI units rather than the CQ effect. This assumption can be supported by the following results. The corresponding low-molecular-weight model compound, M(PMDA/CHA), obtained from PMDA and cyclohexylamine (CHA), had an absorption band peaking at 320 nm with a moderate molar extinction coefficient (ε_{320} = 2400 M^{-1} cm^{-1}) and an absorption tail over 340–370 nm with a low ε (<800 M^{-1} cm^{-1}) [55]. In general, the (π,π*) absorption is an allowed transition with high ε values (>several thousands to 10^4 M^{-1} cm^{-1}), whereas the (n,π*) absorption is a forbidden transition with much lower ε values (<~800 M^{-1} cm^{-1}) [56]. These criteria suggest that the lowest singlet excited state (S$_1$) of the PMDI units is the (n,π*) state. This is probably one reason for why the PMDA/MBCHA film was not highly fluorescent; when the (S$_0$→S$_1$) absorption is a weak transition, its reverse transition (S$_1$→S$_0$ transition, i.e., fluorescence) also necessarily becomes a weak transition. Therefore, if the conjugation in the TCDI units was further extended, the S$_1$ state is expected to change from the (n,π*) state to the (π,π*) state, which significantly enhances the (S$_1$→S$_0$) transition probability (i.e., fluorescence yield).

The PI derived from *s*-BPDA and *trans*-1,4-cyclohexanediamine (*t*-CHDA) with a rigid structure, *s*-BPDA/*t*-CHDA (#16), is a limited PI system that can achieve non-coloration, a very high T_g, and an extremely low CTE [57]. In addition, this PI film exhibited a relatively intense PL spectrum (Φ_{PL} = 0.080) with a peak at 405 nm (Table 3).

A solution of its model compound, M(*s*-BPDA/CHA) [58], showed an absorption band peaking at 325 nm, which was assigned to the (π,π*) transition from its high ε_{325} value (~10,000 M^{-1} cm^{-1}). The fluorescence depolarization measurements of this model compound molecularly dispersed in PMMA solid film also suggested that the 325 nm absorption band corresponds to the S$_1$ state. These results coincide with the fact that the

model compound exhibited an enhanced fluorescence spectrum (Φ_{PL} = 0.04) with a peak at 385 nm in dichloromethane.

The fluorescence spectrum of the *s*-BPDA/*t*-CHDA is slightly red-shifted compared with that of the model compound in solution, suggesting that the former likely differs from the simple fluorescence typical of the "isolated" *s*-BPDI unit. Changing the cycloaliphatic diamine from *t*-CHDA (#16) to MBCHA (#17) and then to M-MBCHA (#18), which enhances the effect of disturbing the chain stacking, appreciably reduced the Φ_{PL}. This implies that the fluorescence emission of the *s*-BPDA/*t*-CHDA film tends to be advantageous owing to the aggregation of the *s*-BPDI units. The fluorescence anisotropy ratio (*r*) measurements of the thick *s*-BPDA/*t*-CHDA film also suggested that the PL spectrum of the *s*-BPDA/*t*-CHDA film likely originates from the BPDI–BPDI ground-state dimer [59]. A similar case is known: poly(ethylene terephthalate) film exhibits fluorescence originating from a ground-state dimer [60]. This hypothesis does not conflict with the following results. The use of an *s*-BPDA isomer, 2,3,3′,4′-BPDA (*a*-BPDA [61]), as well as another isomer, 2,2′,3,3′-BPDA (*i*-BPDA [62,63]), resulted in a significantly weakened PL spectrum (Table 3), probably owing to the prevented BPDI-BPDI stacking as a result of their highly distorted chain structures.

On the other hand, the use of aromatic diamines [i.e., 2,2′-bis(trifluoromethyl)benzidine (TFMB, #19) and *p*-phenylenediamine (*p*-PDA, #20)] resulted in broad and very weak PL spectra in the longer wavelength ranges (>500 nm), which are characteristic of CT fluorescence.

A previous paper [33] reported that the PI derived from hydroquinone diphthalic anhydride (HQDA) and MBCHA exhibited relatively intense PL. The authors also mentioned the contribution of a predicted distorted structure of the HQDA-based diimide (HQDI) units in the PI chains to its PL property. We also measured the PL spectrum of the HQDA/MBCHA film (#23) with the same composition for comparison with the previous data. A similar PL spectrum was observed, except that the Φ_{PL} of our PI film was somewhat lower than the value reported in the literature (Table 3). In addition, we investigated a dilution effect of the HQDI units on the PL yield, using CBDA as an "inert" comonomer diluent. However, decreasing the HQDA content in the HQDA;CBDA/MBCHA copolymer from 100 to 10 and then 2 mol% only slightly enhanced the Φ_{PL}, as shown in Table 3. The observed poor dilution effect (poor CQ effect) is also probably related to the distorted structure of the HQDI units.

p-Phenylenebis(trimellitate anhydride), TA-HQ [64]), in which the ether groups of HQDA are replaced by ester groups, was combined with MBCHA to investigate its PL properties. In contrast to the HQDA-based counterpart, this PI film (#25) was virtually non-fluorescent. Similar non-fluorescent behavior was observed in the related PI (#26) using a TA-HQ analog, *p*-biphenylenebis(trimellitate anhydride), (TA-44BP [65]). These results are likely related to a photo-induced intramolecular CT, as expected from these ester-containing diimide structures, which comprise the electron-donating central aromatic units (*p*-phenylene group for TA-HQ and *p*-biphenylene group for TA-44BP) and electron-accepting trimellitimide unit.

3.1.5. Polyimides Obtained Using Naphthalene-Containing Tetracarboxylic Dianhydrides

We previously systematically investigated the thermal and mechanical properties of wholly aromatic PIs derived from 2,3,6,7-naphthalenetetracarboxylic dianhydride (2,3,6,7-NTDA) and various diamines [66]. As an extension of that research, we earliest reported in 2006 the PL properties of the 2,3,6,7-NTDA-derived PIs and their isomeric system, including their model compounds [41]. In this paper, we show these results in more detail.

The combination of 2,3,6,7-NTDA and *t*-CHDA was expected to afford a colorless PI film with an extremely high T_g and very low CTE owing to its stiff/linear chain structure. However, polyaddition was inhibited by the formation of completely insoluble salt in the initial reaction stage [66]. Instead, the use of MBCHA allowed for the formation of a homogeneous, viscous PAA solution via the gradual dissolution of the initially formed salt and the preparation of a thermally imidized film. The thermal and PL properties of

the 2,3,6,7-NTDA-based PI films are summarized in Table 4. The 2,3,6,7-NTDA/MBCHA film (#27) had a higher T_g (376 °C) and lower CTE (45.2 ppm/K) than those of its PMDA-based counterpart (#14) owing to the linear and planar structure of the 2,3,6,7-NTDA-based diimide (NTDI) unit.

Table 4. PL and thermal properties of polyimides derived from NTDA-based tetracarboxylic dianhydrides with cycloaliphatic or aromatic diamines.

No.	Tetracarboxylic Dianhydride	Diamine	η_{red} (PAA) (dL/g)	T_g (°C)	$T_d{}^5$ (N$_2$) (°C)	$T_d{}^5$ (Air) (°C)	CTE (ppm/K)	λ_{EX} (nm)	λ_{EM} (Peak) (nm)	Φ_{PL}
27		MBCHA	1.94	376	465	403	45.2	350	406	0.014
28	2,3,6,7-NTDA	M-MBCHA	2.00	347	448	381	51.0	350	404	0.021
29		TFMB	2.15	ND	582	559	−3.2	350	510 (CT)	0.0051
30		*p*-PDA	3.21	ND	>590	580	3.1	350	580 (CT)	0.0007
31	CBDA (50) 2,3,6,7-NTDA (50)	MBCHA	0.76	340	432	382	55.6	350	404	0.034
32	CBDA (90) 2,3,6,7-NTDA (10)	MBCHA	0.64	337	420	381	62.6	350	402	0.088
33	CBDA (98) 2,3,6,7-NTDA (2)	MBCHA	0.69	336	427	372	63.6	350	401	0.15
34	CBDA (98) 2,3-NA (4)	MBCHA	1.15	329	427	366	62.3	358	385	0.13
35	CBDA (90) 1,4,5,8-NTDA (10)	MBCHA	0.65	334	426	379	60.7	360	~500	0.0008
36	CBDA (98) 1,8-NA (4)	MBCHA	0.93	350	432	377	65.8	358	422	0.049

Figure 7a shows the PL spectra of 2,3,6,7-NTDA-based PIs using different diamines. The 2,3,6,7-NTDA/MBCHA PI film (#27) exhibited a PL spectrum peaking at 406 nm, probably arising from the local excited state (LE state) of 2,3,6,7-NTDI units in the main chains. The broad emission band appearing at 530 nm is probably due to some NTDI aggregates. However, the LE fluorescence spectrum at 406 nm was much weaker than expected (Φ_{PL} = 0.014, Table 4). On the other hand, the use of M-MBCHA (#28) with bulky methyl side groups, which is expected to more effectively disturb close chain stacking than MBCHA without side groups, significantly enhanced the PL intensity (approximately doubled). This probably reflects the disturbed NTDI-NTDI stacking, and, consequently, a weakened CQ effect. When TFMB, as well as *p*-PDA, was used, the LE fluorescence completely disappeared; instead, a broad, weak PL spectrum characteristic of CT fluorescence was observed in the longer wavelength range.

Figure 7b shows the effect of diluting the 2,3,6,7-NTDI units on the LE fluorescence efficiency. The decrease in 2,3,6,7-NTDA content in the CBDA;2,3,6,7-NTDA/MBCHA copolymers from 100 mol% to 50, 10, and 2 mol% enhanced the Φ_{PL} by approximately tenfold at 2 mol% (Φ_{PL} = 0.15, #33, Table 4), accompanied by the appearance of well-resolved vibronic structures and the disappearance of the broad emission band from the assumed aggregates. The results demonstrate that the PL of the 2,3,6,7-NTDA-based PIs readily undergoes CQ, probably owing to face-to-face NTDI-NTDI stacking.

Copolymerization using 4,4′-(hexafluoroisopropylidene)diphthalic anhydride (6FDA) was reported to be effective in observing the intense PL from the 2,3,6,7-NTDI units [67]; the thermally imidized 6FDA(75 mol%); 2,3,6,7-NTDA(25 mol%)/MBCHA copolymer film prepared by soft-baking at 220 °C showed an intense PL spectrum (Φ_{PL} = 0.2) with a less-resolved vibronic structure compared with those of the afore-mentioned copolymers using CBDA (e.g., 2,3,6,7-NTDA = 2 mol%).
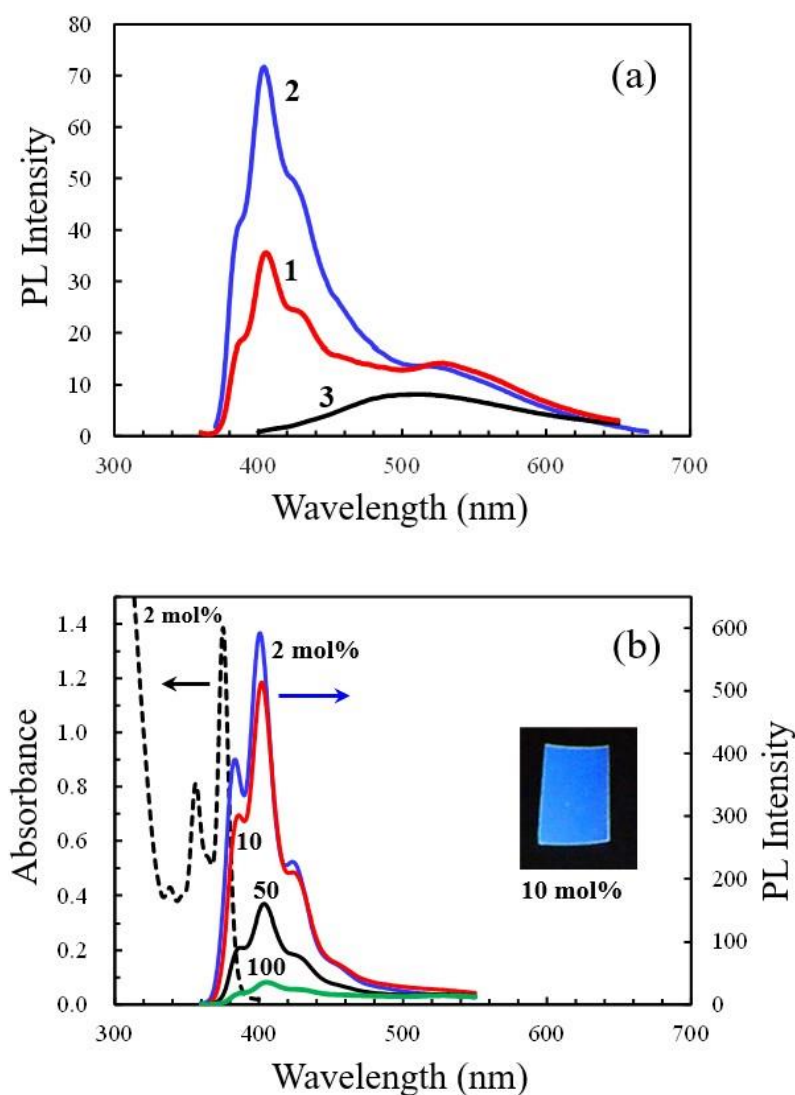
Figure 7. PL spectra of 2,3,6,7-NTDA-based PI films: (**a**) dependence of diamine component (1: MBCHA, 2: M-MBCHA, and 3: TFMB), and (**b**) the dependence on the 2,3,6,7-NTDA content (2, 10, 50, and 100 mol%) in the 2,3,6,7-NTDA;CBDA/MBCHA copolymers. Inset: PL image of the 2,3,6,7-NTDA(10);CBDA(90)/MBCHA copolymer film.

Figure 8a displays the UV-visible absorption and PL spectra of the model compound, M(2,3,6,7-NTDA/CHA), in chloroform at 10^{-5} mol/L. The Φ_{PL} of this solution was 0.162, which can be regarded as the upper limit of that of the corresponding PI film without CQ. The PI film with a sufficiently diluted 2,3,6,7-NTDA content (2 mol%) exhibited a relatively high Φ_{PL} of 0.15, which is close to the value for the dilute solution (Φ_{PL} = 0.162), suggesting that it is difficult to further significantly improve the Φ_{PL} of the optimized 2,3,6,7-NTDA-based PI film (#33).

The UV-visible absorption and PL spectra both have a well-resolved vibronic structure, and a clear mirror image was observed between them. Here, if we used aromatic comonomers instead of CBDA for the dilution of the fluorophore, the resulting UV-visible absorption spectrum would be significantly deformed or masked by the absorption of the host polymers, thereby hindering the observation of the mirror image. The presence of a mirror image provides the following useful photophysical information: in general, the mirror image relationship is satisfied only between the $S_0 \rightarrow S_1$ (absorption) and the $S_1 \rightarrow S_0$ transitions (fluorescence) and only when no structural changes (including internal rotations around single bonds with a conjugation change) occur during the excited-state lifetime (typically in condensed polycyclic aromatic compounds with planar structures

such as benzene, naphthalene, pyrene, anthracene, perylene, etc.). The 2,3,6,7-NTDI unit has a similar planar structure to these condensed aromatic compounds. Accordingly, the observed PL from this model compound corresponds to the $S_1 \rightarrow S_0$ transition (fluorescence). In addition, the 0-0 band at 375 nm in the UV-visible absorption spectrum has a very high ε value (1.04×10^4 M^{-1} cm^{-1}). This magnitude of ε suggests that S_1 is the (π,π^*) state. In addition, a comparison of this model compound with its central unit (i.e., naphthalene) reveals that the former shows a significantly red-shifted absorption spectrum with a higher ε_{max} (1.04×10^4 M^{-1} cm^{-1} at 375 nm) than that of the latter ($\varepsilon_{max} = 5600$ M^{-1} cm^{-1} at 275 nm) [56]. This illustrates that the two imide groups in the 2,3,6,7-NTDI-based model compound, which are connected to the central naphthalene unit, significantly contribute to extending the electronic conjugation.
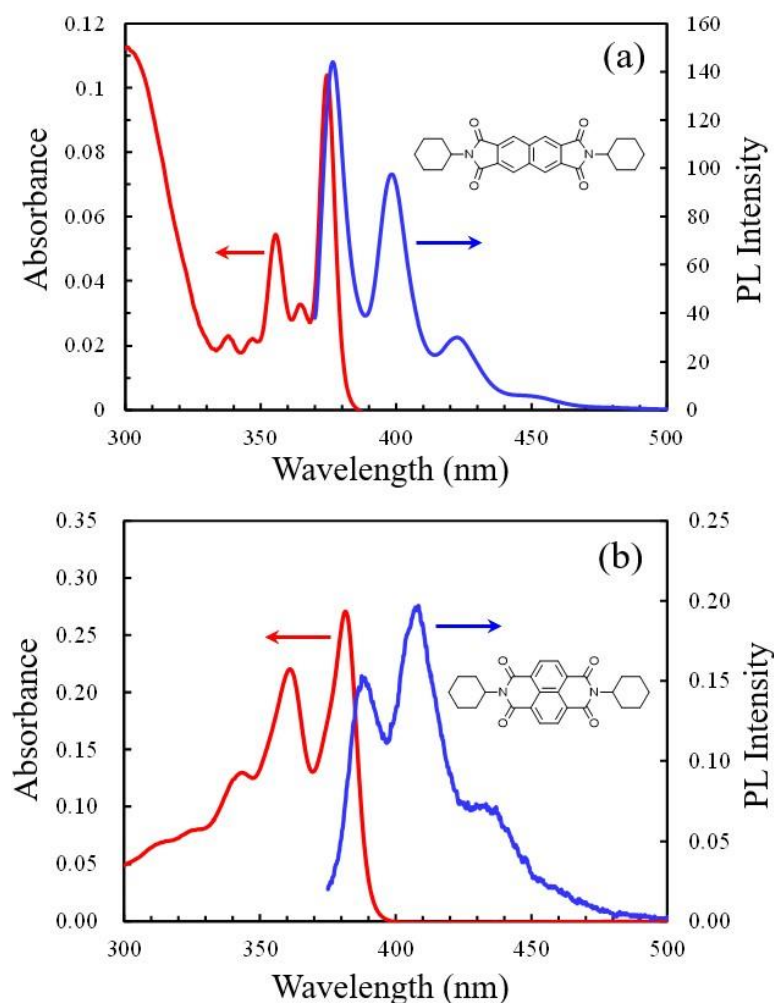
Figure 8. UV-vis absorption (red curves) and PL spectra (blue curves) of NTDA-based model compounds in chloroform (10^{-5} mol/L): (**a**) 2,3,6,7-NTDA system (λ_{EX} = 356 nm) and (**b**) 1,4,5,8-NTDA system (λ_{EX} = 361 nm).

Figure 8b shows the UV-visible absorption and PL spectra of the M(2,3,6,7-NTDA/CHA) isomer, M(1,4,5,8-NTDA/CHA), in chloroform. These spectra have well-resolved vibronic structures with a clear mirror image. The high magnitude of ε_{max} (2.71×10^4 M^{-1} cm^{-1}) at the 0-0 band (382 nm) in the absorption spectrum suggests that S_1 is the (π,π^*) state. Thus, M(1,4,5,8-NTDA/CHA) had spectroscopic parameters similar to those of M(2,3,6,7-NTDA/CHA). Nonetheless, the former was virtually non-fluorescent ($\Phi_{PL} = 0.0014$ at 10^{-6} mol/L) in contrast to the latter. Similarly, a previous paper reported that a M(1,4,5,8-NTDA/CHA) analog, *N,N'*-bis(2,2-dimethylpropyl)-1,4,5,8-naphthaldiimide, was almost non-fluorescent in acetonitrile ($\Phi_{PL} = 0.005$) owing to the involvement of effective intersys-

tem crossing [68]. Based on the results for M(1,4,5,8-NTDA/CHA), the 1,4,5,8-NTDA-based PI films were predicted to be non-fluorescent. Indeed, even the PI film (#35) with a sufficiently diluted 1,4,5,8-NTDA content (10 mol%) was virtually non-fluorescent (Table 4).

In addition, similar results were observed in the terminal-modified PIs using the corresponding mono-functional dicarboxylic acid anhydrides [i.e., 2,3-naphthalenedicarboxylic anhydride (2,3-NA) and 1,8-NA]. The terminal-modified PI with 2,3-NA (#34) exhibited a relatively intense PL (Φ_{PL} = 0.13), as observed for the model compound M(2,3-NA/CHA) (Φ_{PL} = 0.296 in chloroform), corresponding to the 2,3,6,7-NTDA-based systems. By contrast, the terminal-modified PI with 1,8-NA (#36) was less fluorescent (Φ_{PL} = 0.048), as observed for the model compound M(1,8-NA/CHA) (Φ_{PL} = 0.0029 in chloroform), corresponding to the 1,4,5,8-NTDA-based systems. Thus, the observed effect of the imide groups connected at different positions on the PL efficiencies of the PI films was an essential phenomenon.

3.1.6. Polyimides Obtained Using *p*-Terphenylene-Containing Tetracarboxylic Dianhydride

Previous papers reported that combining 3,3″,4,4″-*p*-terphenyltetracarboxylic dianhydride (TPDA) with rigid structures of diamines afforded PI films with ultralow CTEs [57,69]. In addition, the TPDA-based diimide (TPDI) units behaved as a mesogenic structure, and the combinations with flexible diamines including long alkylene groups produced liquid-crystalline PIs [70,71]. A liquid-crystalline PI obtained using TPDA and *s*-BPDA exhibited an intense blue PL, and its EL properties were also reported; however, the PL yields of their solid films and the specific impact of the aggregation of the TPDA-based diimide (TPDI) units on the PL yield were not provided [71]. In the present study, the effects of the cycloaliphatic diamine structure and dilution on the PL efficiency of TPDA-based semi-cycloaliphatic PIs were investigated.

The thermal and PL properties of the TPDA-based PI films are summarized in Table 5. The polyaddition of TPDA and *t*-CHDA proceeded by lightly heating the salt-containing reaction mixture for a short time, and a homogeneous and viscous PAA solution was finally obtained. The thermally imidized film (#37) showed a high T_g (316 °C) and extremely low CTE (8.0 ppm/K). This PI film also exhibited a relatively intense and structureless PL spectrum (Φ_{PL} = 0.15) with a peak at 434 nm, as shown in Figure 9a. The use of MBCHA with a distorted structure (#38), which is more disadvantageous for close chain stacking than *t*-CHDA, resulted in an appreciable enhancement in the PL yield. Interestingly, even when an aromatic diamine (i.e., TFMB) was used, a relatively intense PL spectrum (Φ_{PL} = 0.16) from the LE state occurred without the typical CT fluorescence, as in the TPDA/cycloaliphatic diamine systems. This is in contrast with other TFMB-based PIs (i.e., PMDA/TFMB [72], *s*-BPDA/TFMB and 2,3,6,7-NTDA/TFMB), which exhibit only CT fluorescence. This suggests that the lowest excited state in the TPDA/TFMB system was not the CT state but the LE state of the TPDI unit. However, by replacing TFMB with *p*-PDA, which has a higher electron-donating ability than TFMB, only a very weak CT fluorescence was again observed, whereas the LE fluorescence completely disappeared (Figure 9a).

The fluorophore dilution effect on the PL in the CBDA;TPDA/MBCHA copolymer is shown in Figure 9b. The decrease in TPDA content from 100 mol% to 50 mol% and then to 10 mol% clearly intensified the blue TPDI fluorescence, as evidenced by a high Φ_{PL} of 0.41 for 10 mol% TPDA. However, the dilution effect (CQ effect) observed here was less pronounced than that observed in the 2,3,6,7-NTDA-based PI systems (Figure 7b). This is very likely ascribed to the predicted distorted (non-coplanar) structure of the TPDI units (inset in Figure 9a), which can more effectively disturb the TPDI-TPDI close stacking (contact) underpinning the CQ effect compared with the planar structure of the 2,3,6,7-NTDI units. The presence of the distorted structure in the TPDI units was indicated by the UV-visible absorption and fluorescence spectra, which contained no vibronic structures (Figure 9b). In general, the disappearance of vibronic structures arises when the energy levels of S_0 and S_1 are dispersed by infinitely different extents of conjugation owing to the numerous conformations possible through the internal rotation around single bonds

(with infinitely different dihedral angles), unlike the planar 2,3,6,7-NTDA units without the different conformations.

Table 5. PL and thermal properties of polyimides derived from tetracarboxylic dianhydrides with extended conjugation and cycloaliphatic or aromatic diamines.

No.	Tetracarboxylic Dianhydride (mol%)	Diamine (mol%)	η_{red} (PAA) (dL/g)	T_g (°C)	T_d^5 (N$_2$) (°C)	T_d^5 (Air) (°C)	CTE (ppm/K)	λ_{EX} (nm)	λ_{EM} (Peak) (nm)	Φ_{PL}
37	TPDA	*t*-CHDA	1.17	316	-	-	8.0	350	434	0.15
38		MBCHA	1.16	222	477	444	51.9	350	434	0.26
39		TFMB	1.02	254	591	-	37.2	350	444	0.16
40		*p*-PDA	2.11	ND	-	-	3.0	350	523 (CT)	0.0028
41	CBDA (90) TPDA (10)	MBCHA	1.25	328	432	377	70.8	350	424	0.41
42	CBDA	MBCHA (99.8) PEDI-MBMA (0.2)	1.52	318	428	373	65.3	490	542, 581, 625	0.67
43	CBDA	MBCHA (98) BAPA (2)	0.60	339	438	391	63.1	399	441	0.17
44	HTA-44BP	TFMB (98) BAPA (2)	1.32 (PAA) 0.84 (PI)	265	423	396	69.6	378	436	0.48 (0.804) [a]

[a] Data for the chloroform solution ($c = 26 \times 10^{-4}$ g/mL, $\lambda_{EX} = 375$ nm, Abs = 0.0741 at 375 nm).
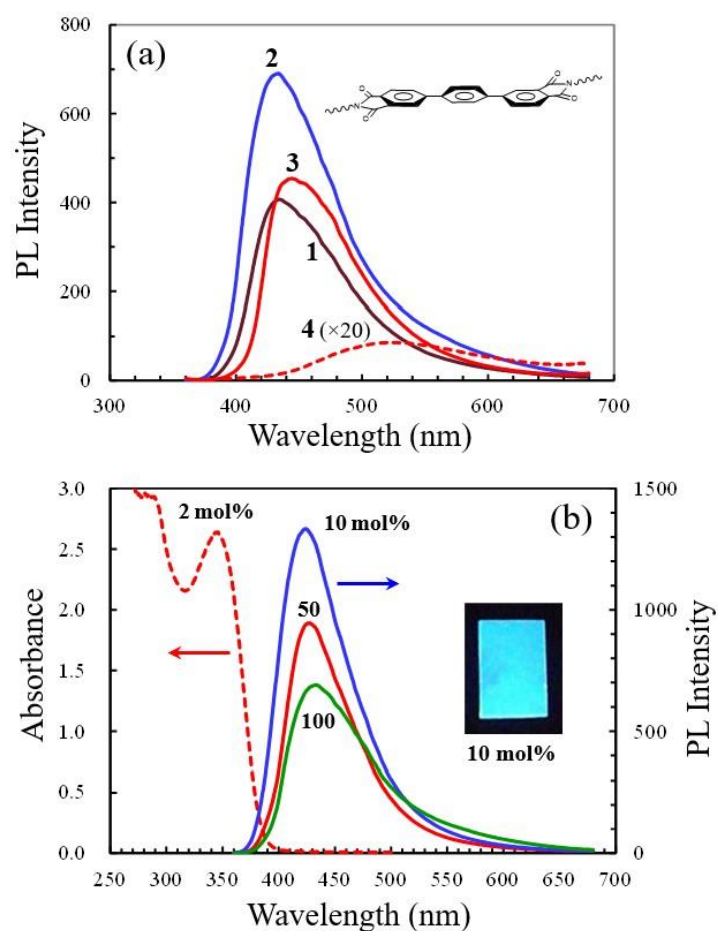
Figure 9. UV-visible absorption and PL spectra of TPDA-based PI films: (**a**) effect of diamine structure (1: *t*-CHDA, 2: MBCHA, 3: TFMB, 4: *p*-PDA (×20)), and (**b**) dependence on the TPDA content (2, 10, 50, and 100 mol%) in the TPDA;CBDA/MBCHA copolymers. Inset: PL image of the TPDA(10);CBDA(90)/MBCHA copolymer film.

3.1.7. Influence of Conjugation in the TCDI Units on the PL Behavior of PI Films

Table 6 summarizes the effects of the character of the lowest excited states, diamine structure, fluorophore concentration, and the ease of the close stacking of the TCDI units on the PL properties. The diagram below the table shows the schematic changes in the energy levels of the lowest excited states, accompanied by the extension of electronic conjugation in the TCDI local structure, by changing the TCDI unit from PMDI to *s*-BPDI, 2,3,6,7-NTDI, and TPDI. As mentioned above, the S_1 (LE) state changed from (n,π*) to (π,π*) by varying the TCDI units from PMDI to *s*-BPDI or 2,3,6,7-NTDI. However, in the wholly aromatic PI systems employing TFMB as the diamine, the lowest excited states remained the CT state; consequently, only CT fluorescence was observed. The use of TPDA with further extended conjugation changed the lowest excited state from CT to LE(π,π*) and, consequently, the TPDI fluorescence was preferentially generated. However, the use of *p*-PDA with a higher electron-donating ability than TFMB once again favored CT fluorescence. Even when *p*-PDA is used as the diamine, there is a chance of preferentially observing intense fluorescence from the LE state if TCDIs with further extended conjugation are selected. For example, the 3,4,9,10-perylenetetracarboxylic dianhydride (PEDA)-based diimide (PEDI) unit may be a candidate if the PEDA/*p*-PDA system could be polymerized.

Table 6. Summary of the S_1 states, the observed PL character, and susceptibility of concentration quenching in the PI films consisting of different aromatic tetracarboxylic dianhydrides (TCDAs) with cycloaliphatic diamines and the related model compounds. The diagram below the table represents the schematic changes in the relative energy levels of the lowest excited states upon extending the conjugation of the TCDI local structures.

TCDA System	S_1 State of CHA-Based Model Compounds in Solution	Effect of Weakened Chain Stacking on PL Yield	Fluorophore Dilution Effect on PL Yield	PL Character of TFMB-Based PIs	PL Character of *p*-PDA-Based PIs
PMDA	(n, π*)	Slight decrease or little change		CT	CT
s-BPDA	(π, π*)	Decrease		CT	CT
2,3,6,7-NTDA	(π, π*)	Some increase	Remarkable enhancement	CT	CT
TPDA	(π, π*)	Some increase	Some increase	LE	CT
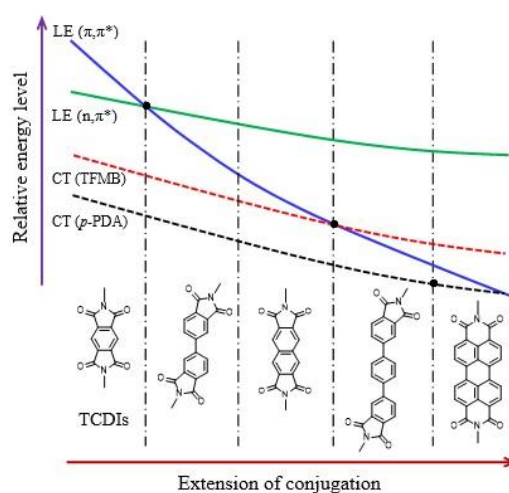
As mentioned above, a prominent fluorophore dilution effect (CQ effect) was observed for the 2,3,6,7-NTDA/cycloaliphatic diamine systems. A similar effect was also observed for its TPDA-based counterparts; however, it was less pronounced than that in the 2,3,6,7-NTDA-based systems. This result very likely reflects the distorted (non-coplanar) local structure of the TPDI units, which can easily disturb the TPDI-TPDI close stacking as the cause of CQ in comparison to its 2,3,6,7-NTDA-based counterpart.

3.1.8. Polyimides Obtained Using Other Monomers with Further Extended Conjugation

A reactive dye, *N*,*N'*-bis[4-(4-amino-3-methylbenzyl)-2-methylphenyl]-3,4,9,10-perylenetetracarboxydiimide (PEDI-MBMA [73]) [Table 7(d)], exhibited a unique feature. The fluorescence of this dye incorporated into the main chains of a wholly aromatic PAA gradually increased with the formation of a lyotropic liquid crystal of this PAA in solution. In the present study, we evaluated the PL yield of a wholly cycloaliphatic PI film modified using a minor content of this dye (0.2 mol%).

Table 7. PL yields of PEDI analogs in DMAc: (a) DBu-PEDI, (b) PEDI-*o*TOL, and (c) PEDI-*o*TOL incorporated in the *s*-BPDA/*p*-PDA-based PAA main chains; (d) PEDI-MBMA, and (e) PEDI-MBMA incorporated in the PAA main chains. PIET: photo-induced electron transfer.
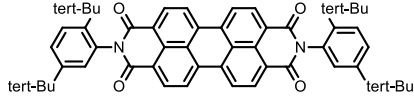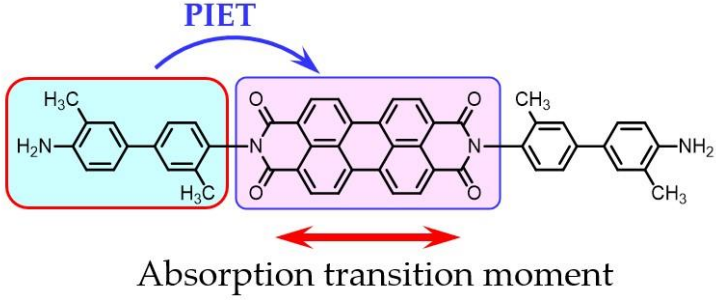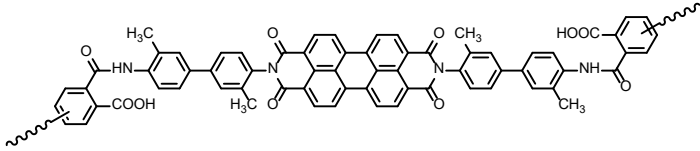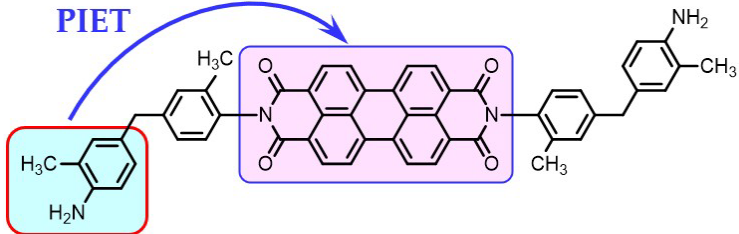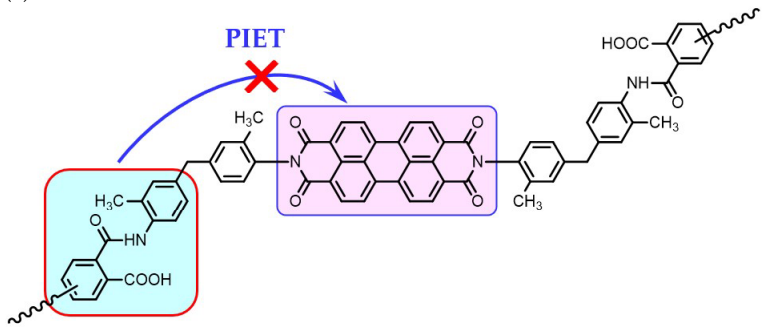
Structures of PEDI Analogs	Φ_{PL}
(a)	0.90
(b)	7.4×10^{-4}
(c)	8.4×10^{-3}
(d)	3.7×10^{-3}
(e)	0.41

Figure 10 shows the UV-visible absorption and PL spectra of the dye-incorporated CBDA/MBCHA-based PI film (#42). A well-resolved vibronic structure and a clear mirror image are apparent in these spectra. This PI film exhibited a very intense green fluorescence in the range of 500–700 nm, with the highest Φ_{PL} (0.67) among the systems examined.
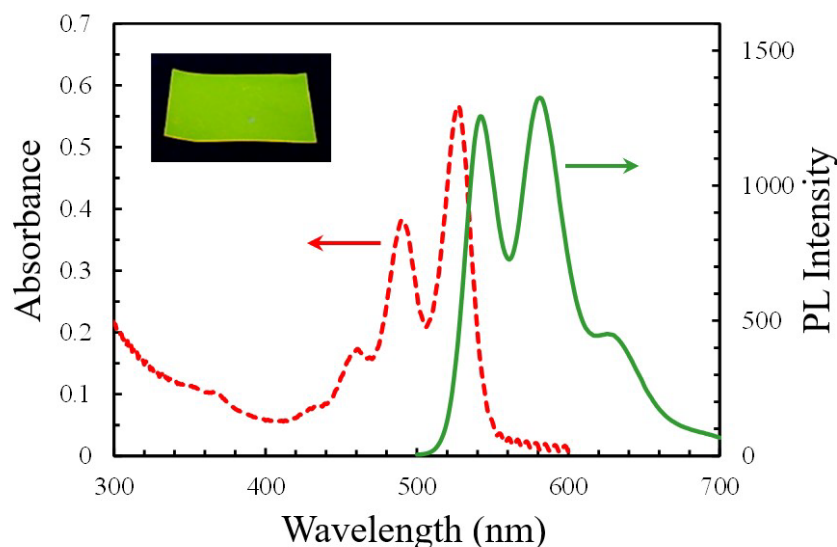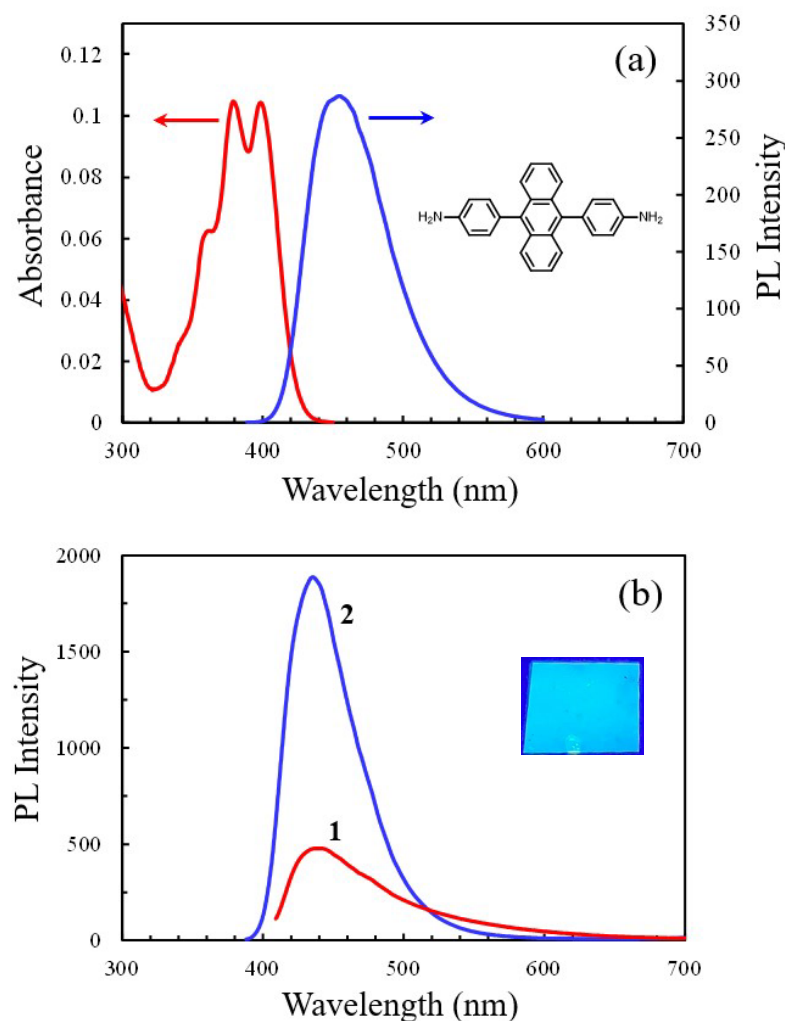

Figure 10. UV-visible absorption and PL spectra of the CBDA/MBCHA(99.8 mol%);PEDI-MBMA(0.2 mol%) copolyimide film. Inset: PL image of the PI film.

In this study, a monomer with further extended conjugation, 9,10-bis(4-aminophenyl) anthracene (BAPA; Figure 6), which includes a *p*-terphenylene substructure analogous to TPDA, was incorporated into cycloaliphatic PIs. The central unit of BAPA, 9,10-diphenylanthracene (DPA), is well known to exhibit an extremely intense blue fluorescence (Φ_{PL} = 0.83 in cyclohexane [74]) with a peak at 430 nm. BAPA, which is the 9,10-diamino-substituted compound of BPA, was also highly fluorescent in chloroform (Φ_{PL} = 0.52), providing a structureless and somewhat red-shifted PL spectrum (λ_{max} = 455 nm) compared with that of BPA (Figure 11a). On the other hand, BAPA showed a UV-visible absorption spectrum with a vibronic structure and a high ε value (1.02×10^4 M^{-1} cm^{-1} at 380 nm) characteristic of the (π,π^*) transition. This relationship (absorption spectrum with a clear vibronic structure and structureless PL spectrum) is probably based on essentially the same mechanism as that observed in the 1-APY solution (Figure 5a); the disappearance of the vibronic structure in the PL spectrum of BAPA likely results from a structural change (internal rotation of the amino groups or 4-aminophenyl groups in BAPA) in solution during its excited-state lifetime.

A previous paper reported that PIs derived from BAPA and an aliphatic TCDA with a spiro structure emitted very intense blue PL (Φ_{PL} = 0.64–0.77) with a λ_{max} of 437–447 nm in DMSO; however, neither the Φ_{PL} values of their solid films nor the specific impact of fluorophore aggregation were provided [30].

In the present study, the PL properties of the CBDA/MBCHA system modified with a minor content of BAPA (2 mol%) were investigated. As shown in Figure 11b, this PI film (#43) exhibited a relatively intense PL spectrum peaking at 441 nm, which was somewhat blue-shifted compared with that of the BAPA monomer in chloroform. However, the Φ_{PL} value (0.17) of this PI film was lower than expected, despite a sufficient dilution of BAPA incorporated into the PI.

Figure 11. UV-visible absorption and PL spectra of BAPA in chloroform (1.00×10^{-5} mol/L) (**a**) and PL spectra of cycloaliphatic copolyimide films modified with BAPA (2 mol%) (**b**): (1) CBDA/MBCHA(98 mol%);BAPA(2 mol%) film prepared via the two-step process and (2) HTA-44BP/TFMB(98 mol%);BAPA(2 mol%) film prepared via chemical imidization. Inset: PL image of the CBDA/MBCHA(98 mol%);BAPA(2 mol%) film (1).

In fact, feasible approaches used to significantly improve this unexpected Φ_{PL} value were very limited. The only conceivable possibility is to alter the chain structures of the host PIs to incorporate the fluorophores. This is because currently using CBDA is advantageous for dense chain stacking owing to its crank-shaft-like rigid steric structure [75]. However, aside from CBDA, there were very few highly reactive cycloaliphatic TCDAs. Recently, we developed a series of novel cycloaliphatic TCDAs, obtained from hydrogenated trimellitic anhydride derivatives (HTA) and various bisphenols. In particular, a TCDA derived from HTA and 4,4′-biphenol (44BP), HTA-44BP (Figure 6), was suitable for producing colorless and solution-processable PIs with high T_g values while avoiding dense chain stacking. For example, the HTA-44BP/TFMB PI achieved an excellent combination of properties: a very high optical transparency (light transmittance at 400 nm: 88.5%), relatively high heat resistance (T_g = 266 °C, T_d^5 (N$_2$) = 423 °C), extremely low water uptake (0.11%), and excellent solution-processability [76]. Based on its excellent solubility, this PI system also had another advantage, i.e., applicability to the chemical imidization process [39], via which the PI film can be formed by simple casting from homogeneous PI solutions at much lower temperatures than those required for the thermal imidization of PAA cast films.

The HTA-44BP/TFMB film modified with BAPA (2 mol%) (#44), prepared via chemical imidization, possessed thermal properties equivalent to those of the original PI, as listed

in Table 5. This solid film (#44) also exhibited a significantly enhanced PL spectrum (Φ_{PL} = 0.48) with a peak at 436 nm. On the other hand, the chloroform solution of this PI had a higher Φ_{PL} (0.80), which can be regarded as the upper limit of the Φ_{PL} value for the BAPA-incorporated PI film samples. Therefore, if an optimal HTA-based PI structure that can further suppress the CQ effect is found, there is a chance of further improving the Φ_{PL}. This effort is currently underway.

3.2. Applications of PEDI Derivatives as Fluorescence Probes

3.2.1. Features of PEDI Fluorescence Behavior

As previously mentioned, non-reactive DBu-PEDI [Table 7(a)] emits considerably intense fluorescence from the LE state of the PEDI unit in DMAc with an extremely high Φ_{PL} of 0.90. The 2-*tert*-butyl groups on the *N,N*′-substituted phenyl groups play an important role in generating this extremely high Φ_{PL}; these bulky substituents not only improve its solubility but also significantly twist the *N*-phenyl groups owing to the steric hindrance between the *tert*-butyl substituents and the adjacent imide C=O groups of the PEDI unit. Consequently, the conjugation between the central PEDI unit and the *N,N*′-phenyl groups, as well as the concomitant PIET toward effective fluorescence quenching, are inhibited. In addition, as reviewed below, DBu-PEDI has unique fluorescence behavior; its fluorescence is intermolecularly effectively quenched by aromatic amide groups (–Ar–CO–NH–Ar′–) in the solid PAA films, whereas almost not quenched by semi-aliphatic amide groups (Ar–CO–NH–Aliph–). In addition, the intermolecular fluorescence quenching effect of the aromatic amide groups is much higher than that of the corresponding imide groups. Therefore, DBu-PEDI dispersed in aromatic PAA films is almost non-fluorescent, but its fluorescence recovers with the progress of imidization. Thus, DBu-PEDI is useful for tracking thermal imidization [77].

Another PEDI analog, *N,N*′-bis[4-(4-amino-3-methylphenyl)-2-methylphenyl]-3,4,9,10-perylenetetracarboxydiimide [PEDI-*o*TOL, Table 7(b)], is a reactive dye with a rod-like structure. This dye, as well as others in the PEDI family, has a considerably intense absorption in the visible range (>500 nm) with a transition moment along its longitudinal direction, which is not masked even by the intense visible CT absorption bands inherent to wholly aromatic PI films. Therefore, the extents of the uniaxial and in-plane chain orientation of PAAs and the corresponding PIs can be indirectly determined from the dichroic ratios of the dye incorporated into their main chains by polarized light absorption measurements. Thus, PEDI-*o*TOL is useful for tracking changes in the chain orientation during thermal imidization [78]. This PEDI dye has another feature: when incorporated into PMDA-based PI main chains, its fluorescence is almost quenched, whereas, when incorporated into other PI systems (e.g., *s*-BPDA-based PI), the PEDI fluorescence recovers. Therefore, this PEDI dye is useful for estimating the miscibility of polymer blends consisting of dye-labeled *s*-BPDA-based PIs and non-labeled PMDA-based PIs; in the miscible state, the PEDI units incorporated into the *s*-BPDA-based PI chains readily have contact with the adjacent PMDA-based PI chains as a quencher, significantly weakening the PEDI fluorescence. In the phase-separated state, the PEDI units incorporated into the *s*-BPDA-based PI chains are separate from the PMDA-based PI chains; consequently, the observed PEDI fluorescence remains intense. This behavior was applicable for evaluating the PI/PI blend miscibility at the molecular level, particularly in the systems consisting of rigid PIs, for which detecting the T_gs is difficult, even using dynamic mechanical analysis [79].

PEDI-*o*TOL itself was non-fluorescent in DMAc, as shown in Table 7(b), very likely owing to PIET (CT) from the electron-donating 4-aminobiphenylene terminal unit to the electron-accepting PEDI unit and subsequent effective non-radiative (thermal) deactivation. When PEDI-*o*TOL was incorporated into the PAA main chains, the PEDI fluorescence from the LE state slightly recovered in the DMAc solution [Table 7(c)]. This is probably attributed to the still-remaining electron-donating ability of the *N*-biphenylene groups, even after the amidation of its terminal amino groups.

A PEDI-*o*TOL analog, PEDI-MBMA [73], also exhibited a non-fluorescent character in DMAc [Table 7(d)] owing to a similar PIET mechanism. However, when PEDI-MBMA was incorporated into the PAA main chains, its PL behavior differed considerably from that of PEDI-*o*TOL; the PEDI fluorescence yield of the former dramatically recovered up to $\Phi_{PL} = 0.41$ by the amidation of its terminal amino groups owing to the significantly reduced electron-donating ability of the *N*-(4-amide-2-methylphenyl) groups formed via the amidation. In this study, this unique property of PEDI-MBMA was harnessed for observing the transamidation of PAAs in solution.

3.2.2. Model Reaction of Transamidation Using PEDI-MBMA

The polymerization of PAAs in solution is an equilibrium reaction comprising the addition reaction of the acid anhydride and amino groups and its reverse reaction, which is, in general, much slower than the forward reaction [4,6,8,13]. In solution, a very small amount of the functional end groups is generated via the partial reverse reaction in the PAA main chains, and they can participate in transamidation via their interdiffusion and subsequent addition with other functional end groups [80]. The equilibrium constants of the polyaddition decrease at higher temperatures, corresponding to the fact that the polyaddition is an exothermic reaction. Therefore, the transamidation as a result of the reverse reaction likely occurs discernibly in an unrefrigerated environment. In a multi-component PAA solution, transamidation can result in the partial formation of a block copolymer, as schematically drawn in Figure 12a.
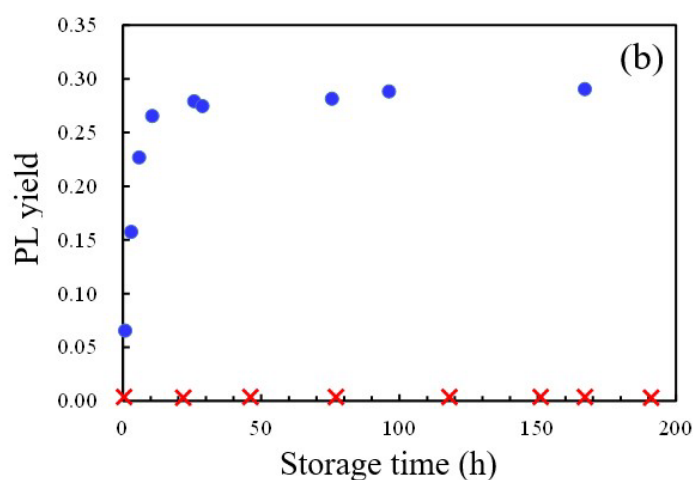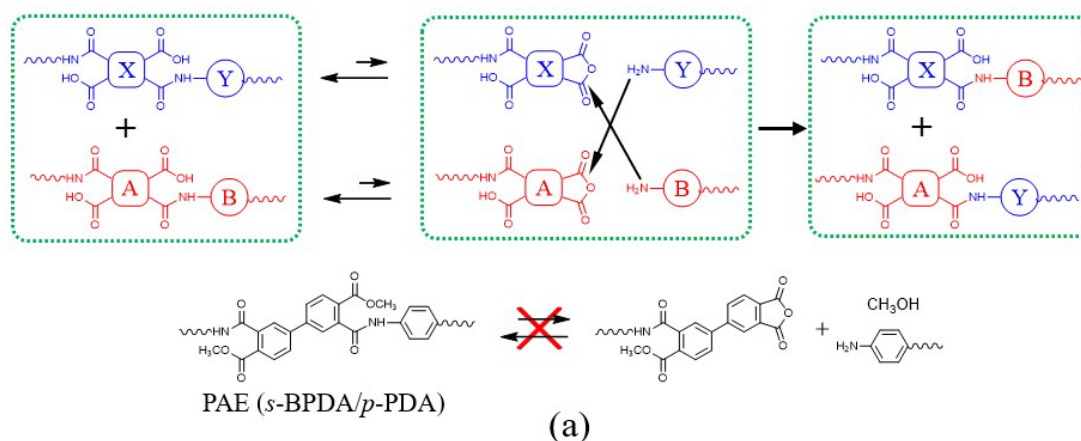
Figure 12. Reaction scheme of transamidation in the PAA solution (**a**) and the results of the model reaction (changes in the PL yield for the PAA solution (solid content: 10 wt%) containing PEDI-MBMA (2.9×10^{-4} mol/L) during storage at 20 °C) (**b**): (●) PAA(*s*-BPDA/*p*-PDA) and (×) PAE.

The potential amidation of the terminal amino groups of PEDI-MBMA in a mixed solution of this reactive dye and a pre-polymerized PAA can be regarded as a model reaction of transamidation. The occurrence of this reaction suggests that transamidation can occur in a real multi-component PAA solution system without this reactive dye. Figure 12b shows the changes in the PEDI fluorescence yield in the mixed solution (solid content: 10 wt%) of PEDI-MBMA and a pre-polymerized PAA (*s*-BPDA/*p*-PDA) or its methyl ester (PAE) during storage in DMAc at 20 °C. In the PAE solution, the PEDI fluorescence yield remained very low during storage, suggesting that no amidation occurred in the terminal amino groups of this reactive dye. This result corresponds to the fact that there is no reverse reaction in PAE in principle (Figure 12a). By contrast, an appreciable increase in the PEDI fluorescence yield was observed in the PAA solution, very likely owing to the amidation of the reactive dye. These results suggest that transamidation can occur in real PAA solutions at unrefrigerated temperatures. Thus, PEDI-MBMA was applicable not only to producing highly photoluminescent PIs but also as a fluorescence probe used to visualize transamidation in the PAA solutions.

4. Conclusions

This study presented heat-resistant polymers exhibiting intense and visible PL. A series of PBOs was polycondensed via the PPA method, and their PL properties were evaluated. The PBO films obtained from aromatic bis(*o*-aminophenol)s and cycloaliphatic dicarboxylic acids did not exhibit intense PL spectra in the visible range, whereas a few wholly aromatic PBO systems were highly photoluminescent. The results suggest that the conjugated 2-PhBO structural units in their main chains are indispensable for producing intense and visible PL. The 6FAP/Bis-B-AF PBO film exhibited the strongest PL (Φ_{PL} = 0.22), peaking at 404/428 nm among the PBOs examined. This probably results from the combined effect of the 2-PhBO units in the main chains and the effectively disturbed CQ in the 2-PhBO units owing to prevented close chain stacking by the high content of bulky HFIP side groups. A PBO system was modified by copolymerization with a minor content of 3,9-PEDCA (1 mol%). The PBO film exhibited an intense green PL (Φ_{PL} = 0.26) peaking at 515 nm.

As a convenient approach used to impart PL functionality to PIs, the chain ends of wholly cycloaliphatic PIs were modified with some conjugated monoamines. For example, the terminal-modified CBDA/MBCHA PI film with 2-AAN exhibited a relatively intense blue PL (Φ_{PL} = 0.12). This simple terminal modification was applied to other heat-resistant polymer systems, PAzMs, which are originally non-photoluminescent. However, the terminal-modified PAzM films with conjugated monoaldehydes (1-PYAL and 9-AAL) remained non-photoluminescent. Thus, this attempt was unsuccessful.

The thermal and PL properties of the PIs derived from 2,3,6,7-NTDA with further extended conjugation were investigated. The 2,3,6,7-NTDA/MBCHA PI film had a high heat resistance and also exhibited purple fluorescence arising from the $S_1(\pi,\pi^*)$ state. However, its Φ_{PL} value was lower than expected. The effect of the dilution of the 2,3,6,7-NTDI units in the PI chains using CBDA on the PL enhancement was pronounced, and, consequently, a relatively high Φ_{PL} (0.15) was obtained at a low 2,3,6,7-NTDA content of 2 mol%. The prominent dilution effect (i.e., CQ effect) is very likely related to the planar structure of the 2,3,6,7-NTDI units, which do not disturb their face-to-face close stacking as the main cause of CQ. By contrast, the counterpart obtained using an 2,3,6,7-NTDA isomer, 1,4,5,8-NTDA, was virtually non-fluorescent, despite the sufficient dilution of the 1,4,5,8-NTDI units using CBDA. The significant isomer effect was confirmed using the corresponding model compounds in solution.

The thermal and PL properties of the counterparts using TPDA with further extended conjugation were evaluated. The TPDA/MBCHA film exhibited an intense blue PL (Φ_{PL} = 0.26) peaking at 434 nm. Dilution with CBDA somewhat intensified its fluorescence, and a very high Φ_{PL} value of 0.41 was achieved at a TPDA content of 10 mol%. However, the observed dilution effect (CQ effect) was less pronounced than that observed for the 2,3,6,7-NTDA-based counterparts. This is reasonably interpreted as the result of the

distorted (non-coplanar) local structure of the TPDI units, which can somewhat disturb their close stacking as the cause of CQ. Interestingly, even when TPDA was combined with an aromatic diamine, TFMB, intense blue fluorescence from the LE state was observed without CT fluorescence. This suggests that its lowest singlet excited state was the LE(π,π^*) state rather than the CT state, owing to the highly extended conjugation in the TPDI units. This study also comprehensively discussed the relationship between the extension of conjugation in the TCDI units and the resultant PL behavior.

The thermally imidized CBDA/MBCHA film modified with a minor content of BAPA (2 mol%) displayed a relatively intense fluorescence ($\Phi_{PL} = 0.17$) peaking at 441 nm. On the other hand, the HTA-44BP/TFMB-based counterpart prepared via chemical imidization resulted in a significant PL enhancement with a considerably high Φ_{PL} of 0.48. This film also had a relatively high heat resistance ($T_g = 265\ °C$ and $T_d{}^5$ (N$_2$) = 423 °C).

A reactive dye, PEDI-MBMA, including the terminal aniline groups, was non-fluorescent in solution owing to PIET from the electron-donating aniline groups to the electron-accepting central PEDI unit and subsequent effective non-radiative deactivation. Nonetheless, the CBDA/MBCHA PI film modified with a minor content of this dye (0.2 mol%) exhibited an extremely intense green fluorescence ($\Phi_{PL} = 0.67$). This reflects the nearly eradicated electron-donating ability of the dye's terminal groups upon conversion from the amino to imide groups during the thermal imidization of the dye-incorporated PAA film.

A similar dramatic change in Φ_{PL} was also observed when this reactive dye was covalently incorporated into the PAA main chains. This unique character was harnessed to observe transamidation between PAAs in solution. In a mixed solution of PAE and PEDI-MBMA, analyzed for comparison, the PEDI fluorescence yield remained very low during storage at 20 °C, suggesting that no amidation occurred in the amino groups of the reactive dye. This result corresponds to the fact that no reverse reaction occurs in PAE in solution in theory. By contrast, an appreciable increase in the PEDI fluorescence yield was observed in the mixed solution of PAA and the reactive dye, reflecting the progress of amidation in the terminal amino groups of the dye. These results suggest that transamidation can occur in real PAA solutions at unrefrigerated temperatures. Thus, PEDI-MBMA was applicable not only to developing highly photoluminescent PIs but also as a fluorescence probe used to visualize the transamidation of PAAs in solution.

Data Availability Statement: The data supporting this study are available within the article and/or its supplementary materials.

Conflicts of Interest: The authors declare no conflict of interest.

References

1. Imai, Y.; Taoka, I.; Uno, K.; Iwakura, Y. Polybenzoxazoles and polybenzothiazoles. *Makromol. Chem.* **1965**, *83*, 167–178. [CrossRef]
2. Cassidy, P.E. *Thermally Stable Polymers: Syntheses and Properties*; Marcel Dekker: New York, NY, USA, 1980.
3. Mittal, K.L. (Ed.) *Polyimides: Synthesis, Characterization, and Applications*; Plenum Press: New York, NY, USA, 1984; Volumes 1–2.
4. Bessonov, M.I.; Koton, M.M.; Kudryavtsev, V.V.; Laius, L.A. (Eds.) *Polyimides: Thermally Stable Polymers*; Plenum: New York, NY, USA, 1987.
5. Feger, C.; Khojasteh, M.M.; McGrath, J.E. (Eds.) *Polyimides: Materials, Chemistry and Characterization*; Elsevier Science Publishers: Amsterdam, The Netherlands, 1989.
6. Sroog, C.E. Polyimide. *Prog. Polym. Sci.* **1991**, *16*, 561–694. [CrossRef]
7. Abadie, M.J.M.; Sillion, B. (Eds.) *Polyimides and Other High-Temperature Polymers*; Elsevier Science Publishers: Amsterdam, The Netherlands, 1991.
8. Bessonov, M.I.; Zubkov, V.A. (Eds.) *Polyamic Acid and Polyimides: Synthesis, Transformation and Structure*; CRC Press: Boca Raton, FL, USA, 1993.
9. Feger, C.; Khojasteh, M.M.; Htoo, M.S. (Eds.) *Advances in Polyimide Science and Technology*; Technomic Publishing: Lancaster, PA, USA, 1993.
10. Ghosh, M.K.; Mittal, K.L. (Eds.) *Polyimides: Fundamentals and Applications*; Marcel Dekker: New York, NY, USA, 1996.
11. Sachdev, H.S.; Khojasteh, M.M.; Feger, C. (Eds.) *Advances in Polyimides and Low Dielectric Polymers*; Society of Plastic Engineers: New York, NY, USA, 1997.
12. Hergenrother, P.M. The use, design, synthesis, and properties of high performance/high temperature polymers: An overview. *High Perform. Polym.* **2003**, *15*, 3–45. [CrossRef]
13. Ando, S.; Ueda, M.; Kakimoto, M.; Kochi, M.; Takeichi, T.; Hasegawa, M.; Yokota, R. (Eds.) *The Latest Polyimides: Fundamentals and Applications*, 2nd ed.; NTS: Tokyo, Japan, 2010.
14. Liaw, D.J.; Wang, K.L.; Huang, Y.C.; Lee, K.R.; Lai, J.Y.; Ha, C.S. Advanced polyimide materials: Syntheses, physical properties and applications. *Prog. Polym. Sci.* **2012**, *37*, 907–974. [CrossRef]
15. Tsai, C.L.; Yen, H.J.; Liou, G.S. Highly transparent polyimide hybrids for optoelectronic applications. *React. Funct. Polym.* **2016**, *108*, 2–30. [CrossRef]
16. Yang, C.Y. (Ed.) *Advanced Polyimide Materials: Synthesis, Characterization, and Applications*; Chemical Industry Press: Shanghai, China; Elsevier: Amsterdam, The Netherlands, 2018.
17. Diaham, S. (Ed.) *Polyimide for Electronic and Electrical Engineering Applications*; IntechOpen: London, UK, 2021.
18. Fukukawa, K.; Ueda, M. Recent development of photosensitive polybenzoxazoles. *Polym. J.* **2006**, *38*, 405–418. [CrossRef]
19. Fukukawa, K.; Ueda, M. Recent progress of photosensitive polyimides. *Polym. J.* **2008**, *40*, 281–296. [CrossRef]
20. Freilich, S.C. Photoconductivity of donor-loaded polyimides. *Macromolecules* **1987**, *20*, 973–978. [CrossRef]
21. Jeong, K.M.; Tapaswi, P.K.; Kambara, T.; Ishige, R.; Ando, S.; Ha, C.S. Photoconductive polyimides derived from a novel imid-azole-containing diamine. *High Perform. Polym.* **2020**, *32*, 620–630. [CrossRef]
22. Zhang, Q.; Tsai, C.Y.; Li, L.J.; Liaw, D.J. Colorless-to-colorful switching electrochromic polyimides with very high contrast ratio. *Nat. Commun.* **2019**, *10*, 1239. [CrossRef]
23. Kim, D.Y.; Cho, H.N.; Kim, C.Y. Blue light emitting polymers. *Prog. Polym. Sci.* **2000**, *25*, 1089. [CrossRef]
24. Ghassemi, H.; Zhu, J.H. Fluorescence of perylene- and naphthalene-containing polyimides: Evidence of molecular aggregation and chain coiling in chloroform solution. *J. Polym. Sci. Part B Polym. Phys.* **1995**, *33*, 1633–1639. [CrossRef]
25. Li, W.; Fox, M.A. Photophysical and photochemical properties of anthryl-labeled polyimides: Fluorescence, electron transfer, and photoreaction. *J. Phys. Chem. B* **1997**, *101*, 11068–11076. [CrossRef]
26. Pyo, S.M.; Kim, S.I.; Shin, T.J.; Ree, M.; Park, K.H.; Kang, J.S. Synthesis and blue light-emitting characteristic of rod-like poly(4,4′-biphenylene pyromellitimide) with fury1 side groups. *Polymer* **1998**, *40*, 125–130. [CrossRef]
27. Pyo, S.M.; Kim, S.I.; Shin, T.J.; Park, H.K.; Ree, M.; Park, K.H.; Kang, J.S. Synthesis and characterization of a new blue-light-emitting polyimide. *Macromolecules* **1998**, *31*, 4777–4781. [CrossRef]
28. Mal'tsev, E.I.; Brusentseva, M.A.; Lypenko, D.A.; Berendyaev, V.I.; Kolesnikov, V.A.; Kotov, B.V.; Vannikov, A.V. Electroluminescent properties of anthracene-containing polyimides. *Polym. Adv. Technol.* **2000**, *11*, 325–329. [CrossRef]
29. Huang, W.; Yan, D.; Lu, Q.; Huang, Y. Synthesis and characterization of highly soluble fluorescent main chain copolyimides containing perylene units. *Eur. Polym. J.* **2003**, *39*, 1099–1104. [CrossRef]
30. Kudo, K.; Imai, T.; Hamada, T.; Sakamoto, S. Synthesis of blue emitting alicyclic polyimides using one-pot alternating copolymerization method. *High Perform. Polym.* **2006**, *18*, 749–759. [CrossRef]
31. Ishizaka, T.; Kasai, H.; Oikawa, H.; Nakanishi, H. Unique luminescence properties of Eu^{3+}-doped polyimide. *J. Photochem. Pho-tobiol. A Chem.* **2006**, *183*, 280–284. [CrossRef]
32. Wu, J.H.; Liou, G.S. High-efficiency fluorescent polyimides based on locally excited triarylamine-containing dianhydride moieties. *Polym. Chem.* **2015**, *6*, 5225–5232. [CrossRef]
33. Wakita, J.; Sekino, H.; Sakai, K.; Urano, Y.; Ando, S. Molecular design, synthesis, and properties of highly fluorescent polyimides. *J. Phys. Chem. B* **2009**, *113*, 15212–15224. [CrossRef] [PubMed]

34. Kanosue, K.; Hirata, S.; Vacha, M.; Augulis, R.; Gulbinas, V.; Ishige, R.; Ando, S. A colorless semi-aromatic polyimide derived from a sterically hindered bromine-substituted dianhydride exhibiting dual fluorescence and phosphorescence emission. *Mater. Chem. Front.* **2019**, *3*, 39–49. [CrossRef]

35. Liang, N.; Fujiwara, E.; Nara, M.; Ishige, R.; Ando, S. Colorless copolyimide films exhibiting large stokes-shifted photoluminescence applicable for spectral conversion. *ACS Appl. Polym. Mater.* **2021**, *3*, 3911–3921. [CrossRef]

36. Tabuchi, A.; Hayakawa, T.; Kuwata, S.; Ishige, R.; Ando, S. Synthesis and characterization of white-light luminescent end-capped polyimides based on FRET and excited state intramolecular proton transfer. *Polymers* **2021**, *13*, 4050. [CrossRef]

37. Ando, S. Characteristic changes in the structures and properties of polyimides induced by very high pressures up to 8 GPa. *Polym. J.* **2023**, *2023*, 1–8. [CrossRef]

38. Hasegawa, M.; Horie, K. Photophysics, photochemistry, and optical properties of polyimides. *Prog. Polym. Sci.* **2001**, *26*, 259–335. [CrossRef]

39. Hasegawa, M. Development of solution-processable, optically transparent polyimides with ultra-low linear coefficients of thermal expansion. *Polymers* **2017**, *9*, 520. [CrossRef]

40. Hasegawa, M.; Ichikawa, K.; Takahashi, S.; Ishii, J. Solution-processable colorless polyimides derived from hydrogenated pyromellitic dianhydride: Strategies to reduce the coefficients of thermal expansion by maximizing the spontaneous chain orientation behavior during solution casting. *Polymers* **2022**, *14*, 1131. [CrossRef]

41. Horii, S.; Hasegawa, M. Photoluminescent high-temperature polymers (6). Polyimides, polybenzoxazoles, and polyazomethines. *Polym. Prepr. Jpn.* **2006**, *55*, 4089.

42. Nitta, H.; Hasegawa, M. Photoluminescent high-temperature polymers (9). Highly blue-fluorescent soluble polyimides. *Polym. Prepr. Jpn.* **2008**, *57*, 4183.

43. Etienne, A.; Arcos, J.C. ms-Bis(aminophenyl)anthradiols. I. ms-Bis(*p*-dialkylaminophenyl)anthradiols. *Bull. Soc. Chim. Fr.* **1951**, *236*, 727–732.

44. Popp, F.D.; McEwen, W.E. Polyphosphoric acid as a reagent in organic chemistry. *Chem. Rev.* **1958**, *58*, 321–401. [CrossRef]

45. Birks, J.B. Fluorescence quantum yield measurements. *J. Res. Natl. Bur. Stand.* **1976**, *80A*, 389–399. [CrossRef] [PubMed]

46. Ford, W.E.; Kamat, P.V. Photochemistry of 3,4,9,10-perylenetetracarboxylic dianhydride dyes. 3. Singlet and triplet excited-state properties of the bis(2,5-di-tert-butylphenyl)imide derivative. *J. Phys. Chem.* **1987**, *91*, 6373–6380. [CrossRef]

47. Miyazaki, T.; Hasegawa, M. Highly Tough and Highly Transparent Soluble Polybenzoxazoles. *High Perform. Polym.* **2007**, *19*, 243–269. [CrossRef]

48. Chou, P.T.; Cooper, W.C.; Clements, J.H.; Studer, S.L.; Chang, C.P. A comparative study. The photophysics of 2-phenylbenzoxazoles and 2-phenylbenzothiazoles. *Chem. Phys. Lett.* **1993**, *216*, 300–304. [CrossRef]

49. Bains, G.; Patel, A.B.; Narayanaswami, V. Pyrene: A probe to study protein conformation and conformational changes. *Mole-cules* **2011**, *16*, 7909–7935. [CrossRef]

50. Barik, S.; Skene, W.G. Turning-on the quenched fluorescence of azomethines through structural modifications. *Eur. J. Org. Chem.* **2013**, *2013*, 2563–2572. [CrossRef]

51. Kaya, I.; Yıldırım, M.; Avcı, A. Synthesis and characterization of fluorescent polyphenol species derived from methyl substitut-ed aminopyridine based Schiff bases: The effect of substituent position on optical, electrical, electrochemical, and fluorescence properties. *Synth. Met.* **2010**, *160*, 911–920. [CrossRef]

52. Yoshino, J.; Kano, N.; Kawashima, T. Fluorescence properties of simple *N*-substituted aldimines with a B-N interaction and their fluorescence quenching by a cyanide ion. *J. Org. Chem.* **2009**, *74*, 7496–7503. [CrossRef]

53. Ishii, J.; Oshima, N.; Tanaka, Y.; Hasegawa, M. Film properties of polyazomethines (1). Effect of incorporation of iintramolecular cyclodehydrating uunits. *High Perform. Polym.* **2010**, *22*, 259–273. [CrossRef]

54. Morgan, P.W.; Kwolek, S.L.; Pletcher, T.C. Aromatic azomethine polymers and fibers. *Macromolecules* **1987**, *20*, 729–739. [CrossRef]

55. Ishida, H.; Wellinghoff, S.T.; Baer, E.; Koenig, J.L. Spectroscopic studies of poly[*N*,*N*′-bis(phenoxyphenyl)pyromellitimide]. 1. Structures of the polyimide and three model compounds. *Macromolecules* **1980**, *13*, 826–834. [CrossRef]

56. Rao, C.N.R. Ultra-violet and visible spectroscopy. In *Chemical Applications*, 2nd ed.; Butterworth & Co.: London, UK, 1967.

57. Hasegawa, M.; Koyanaka, M. Polyimides containing trans-1,4-cyclohexane unit. Polymerizability of their precursors and low-CTE, low-*k* and high-*T*$_g$ properties. *High Perform. Polym.* **2003**, *15*, 47–64. [CrossRef]

58. Hasegawa, M.; Shindo, Y.; Sugimura, T.; Ohshima, S.; Horie, K.; Kochi, M.; Yokota, R.; Mita, I. Photophysical processes in ar-omatic polyimides. Studies with model compounds. *J. Polym. Sci. Part B Polym. Phys.* **1993**, *31*, 1617–1625. [CrossRef]

59. Ishii, J.; Horii, S.; Sensui, N.; Hasegawa, M.; Vladimirov, L.; Kochi, M.; Yokota, R. Polyimides containing trans-1,4-cyclohexane unit (III). Ordered structure and intermolecular interaction in *s*-BPDA/CHDA polyimide. *High Perform. Polym.* **2009**, *21*, 282–303. [CrossRef]

60. Hemker, D.J.; Frank, C.W.; Thomas, J.W. Photophysical studies of amorphous orientation in poly(ethylene terephthalate) films. *Polymer* **1988**, *29*, 437–447. [CrossRef]

61. Hasegawa, M.; Sensui, N.; Shindo, Y.; Yokota, R. Structure and properties of novel asymmetric biphenyl-type polyimides. Ho-mo- and copolymers and blends. *Macromolecules* **1999**, *32*, 387–396. [CrossRef]

62. Tong, Y.; Huang, W.; Luo, J.; Ding, M. Synthesis and properties of aromatic polyimides derived from 2,2′,3,3′-biphenyltetracarboxylic dianhydride. *J. Polym. Sci. Part A Polym. Chem.* **1999**, *37*, 1425–1433. [CrossRef]

63. Rozhanskii, I.; Okuyama, K.; Goto, K. Synthesis and properties of polyimides derived from isomeric biphenyltetracarboxylic dianhydrides. *Polymer* **2000**, *41*, 7057–7065. [CrossRef]

64. Hasegawa, M.; Koseki, K. Poly(ester imide)s possessing low CTE and low water absorption. *High Perform. Polym.* **2006**, *18*, 697–717. [CrossRef]

65. Hasegawa, M.; Hirai, T.; Ishigami, T.; Takahashi, S.; Ishii, J. Optically transparent aromatic poly(ester imide)s with low coeffi-cients of thermal expansion (2) Effect of introduction of alkyl-substituted *p*-biphenylene units. *Polym. Int.* **2018**, *67*, 431–444. [CrossRef]

66. Hasegawa, M.; Horii, S. Low-CTE polyimides derived from 2,3,6,7-naphthalenetetracarboxylic dianhydride. *Polym. J.* **2007**, *39*, 610–621. [CrossRef]

67. Doi, M.; Muto, K.; Nara, M.; Liang, N.; Sano, K.; Mori, H.; Ishige, R.; Ando, S. Photoluminescence properties of copolyimides containing naphthalene core and analysis of excitation energy transfer between the dianhydride moieties. *J. Photopolym. Sci. Technol.* **2021**, *34*, 423–430. [CrossRef]

68. Aveline, B.M.; Matsugo, S.; Redmond, R.W. Photochemical mechanisms responsible for the versatile application of naph-thalimides and naphthaldiimides in biological systems. *J. Am. Chem. Soc.* **1997**, *119*, 11785–11795. [CrossRef]

69. Ueshima, K.; Kikuchi, T. Some properties of polyimides derived from *p*- or *m*-terphenyltetracarboxylic dianhydride. *Polym. Prepr. Jpn.* **1990**, *39*, 796–798.

70. Inoue, T.; Kakimoto, M.; Imai, Y.; Watanabe, J. First observation of a thermotropic liquid crystal in a simple polyimide derived from 1,11-diaminoundecane and 4,4′-terphenyltetracarboxylic acid. *Macromolecules* **1996**, *28*, 6368–6370. [CrossRef]

71. Sato, M.; Nakamoto, Y.; Yonetake, K.; Kido, J. Preparation, thermotropic liquid-crystalline and fluorescent properties of semi-rigid homo- and copoly(ester-imide)s composed of 3,3″,4,4″-*p*-terphenyltetracarboxdiimide and 3,3′,4,4′-biphenyltetracarboxdiimide. *Polym. J.* **2002**, *34*, 601–607. [CrossRef]

72. Ishii, J.; Takata, A.; Oami, Y.; Yokota, R.; Vladimirov, L.; Hasegawa, M. Spontaneous molecular orientation of polyimides in-duced by thermal imidization (6). Mechanism of negative in-plane CTE generation in non-stretched polyimide films. *Eur. Polym. J.* **2010**, *46*, 681–693. [CrossRef]

73. Ebisawa, S.; Ishii, J.; Sato, M.; Vladimirov, L.; Hasegawa, M. Spontaneous molecular orientation of polyimides induced by thermal imidization (5). Effect of ordered structure formation in polyimide precursors on CTE. *Eur. Polym. J.* **2010**, *46*, 283–297. [CrossRef]

74. Demas, J.N.; Crosby, G.A. The measurement of photoluminescence quantum yields. A review. *J. Phys. Chem.* **1971**, *75*, 991–1024.

75. Suzuki, H.; Abe, T.; Takaishi, K.; Narita, M.; Hamada, F. The synthesis and X-ray structure of 1,2,3,4-cyclobutane tetracarbox-ylic dianhydride and the preparation of a new type of polyimide showing excellent transparency and heat resistance. *J. Polym. Sci. Part A Polym. Chem.* **2000**, *38*, 108–116. [CrossRef]

76. Hasegawa, M.; Kasamatsu, K.; Koseki, K. Colorless poly(ester imide)s derived from hydrogenated trimellitic anhydride. *Eur. Polym. J.* **2012**, *48*, 483–498. [CrossRef]

77. Hasegawa, M.; Ishii, J.; Shindo, Y. Unique fluorescence behavior of perylenetetracarboxydiimides in polyimide systems. *J. Polym. Sci. Part B Polym. Phys.* **1998**, *36*, 827–840. [CrossRef]

78. Ishii, J.; Shimizu, N.; Ishihara, N.; Ikeda, Y.; Sensui, N.; Matano, T.; Hasegawa, M. Spontaneous molecular orientation of polyi-mides induced by thermal imidization (4). Casting- and melt-induced in-plane orientation. *Eur. Polym. J.* **2010**, *46*, 69–80. [CrossRef]

79. Hasegawa, M.; Ishii, J.; Shindo, Y. Polyimide/Polyimide blend miscibility probed by perylenetetracarboxydiimide fluorescence. *Macromolecules* **1999**, *32*, 6111–6119. [CrossRef]

80. Kreuz, J.A.; Coff, D.L. *Materials Science of High Temperature Polymers for Microelectronics (Materials Research Society Symposium Proceedings)*; Grubb, D.T., Mita, I., Yoon, D.Y., Eds.; Materials Research Society: Pittsburgh, PA, USA, 1991; Volume 227, p. 11.